47p

N63 16160

NASA TN D-1637

NASA TN D-1637

codes

TECHNICAL NOTE

D-1637

QUALITATIVE EVALUATION OF EFFECT OF HELICOPTER ROTOR-BLADE TIP VORTEX ON BLADE AIRLOADS

By James Scheiman and LeRoy H. Ludi

Langley Research Center
Langley Station, Hampton, Va.

NATIONAL AERONAUTICS AND SPACE ADMINISTRATION

WASHINGTON May 1963

NATIONAL AERONAUTICS AND SPACE ADMINISTRATION

TECHNICAL NOTE D-1637

QUALITATIVE EVALUATION OF EFFECT OF HELICOPTER ROTOR-BLADE TIP VORTEX ON BLADE AIRLOADS

By James Scheiman and LeRoy H. Ludi

SUMMARY

A flight test program was conducted to determine both representative and critical helicopter rotor-blade airloads by means of 49 pressure transducers in the blade.

Two flight conditions are examined in detail. A comparison is made of the measured results and the results from uniform inflow theory. Important differences that exist are shown to occur near the intersection of the blade with the path of the preceding blade tip and thus can be attributed to the blade trailing vortices. The vibratory blade loading is shown to be significantly influenced by the trailing vortex of the preceding blades. This influence produces harmonic blade loadings of all orders, and the percentage of the contribution to the higher harmonics is large.

Theoretical and experimental chordwise pressure distributions are compared and the results indicate that the differences are due to inflow or blade angle of attack and not to other effects (e.g., unsteady state flow).

Sample oscillograph records for other flight conditions are presented to show the influence of the tip vortex on the blade loading.

INTRODUCTION

Vibratory loads are one of the major helicopter problems both in respect to structural fatigue and acceptable fuselage vibration levels. The ability to effectively predict these loads has long been an objective, both to permit a study of means to reduce them and to shorten the development span for new designs. Assumptions which are entirely adequate for performance prediction do not take account of load distribution to an extent usable for periodic load prediction. While helicopter dynamic analysis has improved significantly and numerous attempts have been made to improve the accuracy of predicting vibratory airloads, the net results have been limited. A shortage of experimental information on the periodic airloads has seemed the major impediment to the devising of adequate theory for

steady flight conditions; and the maneuver and vortex-ring flight conditions must be expected to require semiempirical approaches.

In order to help fill this gap, the National Aeronautics and Space Administration has flight tested a single-rotor helicopter equipped with extensive instrumentation. Numerous blade span and chord pressure sensors, blade motions and stress, and flight variables were recorded and the data reduced. In this report a small portion of these data is used to illustrate an initial finding of practical interest.

A comparison of the measured blade loads with the loads predicted by elementary uniform inflow theory indicated a predominant influence of the blade tip vortices. The determination of the actual tip-vortex position, motion, and strength is a difficult problem. Also, in forward flight the blade spanwise loading and the shed and trailing vortices vary with time.

Regardless of the status of numerical solutions, however, a qualitative picture is believed to be an important aid to understanding. This report presents such a qualitative evaluation of the tip-vortex influence on the rotor-blade airloads, based on the recorded flight measurements. A detailed evaluation is made for two trim level-flight conditions, one with and one without retreating blade stall. For completeness and in order to provide useful data to supplement the work of other researchers, a portion of the reduced data and the flight conditions are included in the appendix for the two level-flight conditions considered herein and one additional flight condition. Sample oscillograph records of numerous other flight conditions are offered as further evidence of the presence of the tip-vortex effect.

SYMBOLS

c airfoil chord, in.

C_N normal-force coefficient, $\int_0^{1.0} \frac{-\Delta p}{q} \, d\left(\frac{x}{c}\right)$

Δp pressure difference between upper and lower surfaces of blade, lb/sq in.

q dynamic pressure, lb/sq in.

r spanwise distance along radius measured from center of rotation, in.

R blade radius measured from center of rotation, in. or ft

V rotor forward velocity, ft/sec

x chordwise distance from airfoil leading edge, in.

α rotor angle of attack; angle between flight path and plane perpendicular to axis of no feathering, positive when axis is pointing rearward, radians

μ rotor tip-speed ratio, $\frac{V \cos \alpha}{\Omega R}$

ψ azimuth angle of rotor blade including lagging motion, measured in direction of rotation from downwind position, deg

ψ_{nom} azimuth angle of rotor blade without any lagging motion, measured in direction of rotation from downwind position, deg

Ω rotor angular velocity, radians/sec

DESCRIPTION OF EQUIPMENT AND DATA PRESENTATION

Description of Equipment

The single-rotor helicopter used in the present investigation is shown in figure 1, and its principal dimensions and approximate physical characteristics are listed in table I. The rotor is equipped with four fully articulated blades each having a planform as shown in figure 2 and each equipped with offset flapping and drag hinges. The rotor blade has stiffness and weight distributions as shown in figure 2. The rotor is a standard production rotor modified only to the extent required for the necessary instrumentation. The blade is constructed with a full-span trailing-edge tab. The tab is deflected upward 4° from $r/R = 0.85$ to $r/R = 0.90$.

Two-dimensional wind-tunnel model tests were performed to obtain airfoil characteristic data. These results are reported in reference 1.

The pressure transducers used are NASA miniature electrical pressure gages of the type described in reference 2. Forty-nine gages are mounted inside one rotor blade in such a way that neither centrifugal force nor flapping accelerations affect gage output. A sample of the pressure-gage installation in the blade is shown in figure 3. The 49 gages are distributed over the blade in the chordwise and the radial directions as indicated in table II. Each gage is connected to the appropriate pair of orifices by tubing having an inside diameter of 0.04 inch. The tubing length is constant for all gages in order to maintain constant amplitude and phase response between gages. The electrical output from all the pressure transducers was simultaneously recorded on oscillographs through the use of a 160 slip-ring assembly. In addition, the slip rings permit the simultaneous recording of blade flapwise bending, chordwise bending, and torsional moments and the blade pitching, flapping, and lagging motions.

Records of the standard flight parameters were obtained by the use of standard NASA recording instruments having synchronized time scales which measure airspeed, altitude, manifold pressure, rotor rotational speed, pilot-control positions, angular velocities about the three principal inertia axes, and helicopter center-of-gravity acceleration. Most of these data are not pertinent to the present discussion and therefore are not included herein.

Analysis and Data Presentation

Tables III, IV, and V present a portion of the data obtained and reduced in the flight test program. Each data point presented is an average of three oscillograph record points taken in three consecutive rotor revolutions. At selected portions of the oscillograph film, the trace deflections were read with the use of a telereader. These results were recorded on IBM punch cards which were processed through an IBM 7070 electronic data processing system and the final results tabulated.

The data analyzed and discussed in this report are for two level-flight conditions with tip-speed ratios of 0.18 and 0.23, without and with retreating blade stall, respectively. Further flight-condition details and the accuracy of the data can be obtained in the appendix. Illustrated graphical data are shown in figures 4 to 14.

RESULTS AND DISCUSSION

The data discussed herein are restricted to three outboard blade stations for an unstalled condition at $\mu = 0.18$ and for a stalled condition at $\mu = 0.23$. A comparison is made of the measured blade loads and loads calculated from uniform inflow theory, and a qualitative treatment of the differences between measured and calculated loads is presented.

Unstalled Blade Section ($\mu = 0.18$)

Chord section loading.- Figure 4 presents the blade section loading per unit span as a function of the azimuth angle for three radius stations. The measured data were obtained from a numerical integration of the differential pressure gages. The calculated results are based on a rigid blade with a uniform inflow, two-dimensional airfoil characteristics, and the first three harmonics of measured blade lead-lag, flapping, and pitch motions. For this report, the most interesting parts of these plots are the "jumps" that appear in the measured section loading data at azimuth angles near 90° and 270°; however, these jumps are not in the calculated curves. It is shown that these jumps are caused by the intersection of the instrumented blade with the trailing vortex shed from the tip of leading blades; this effect is not accounted for in uniform inflow theory.

Blade tip path.- Figure 5 is a plot of the blade tip path of two succeeding rotating blades with the center of rotation in linear motion (forward flight $\mu = 0.18$). From this figure the spanwise intersection point of the following blade (instrumented blade) with the tip path of the leading blade can be determined. Figure 6 is a plot of this radial intersection point as a function of the azimuth angle of the following blade. With a fixed blade radial station given (e.g., the location of the pressure gages), the azimuth angle at which these fixed points on the following blade strike the tip path traveled by the leading blade can be determined from figure 6. These intersection points are indicated by vertical lines or ticks in figure 4. It is seen that the ticks occur in the neighborhood of the jumps in the measured chord section loading.

Blade tip vortex.- Because the blade lift distribution varies with radius and with time, a vortex sheet is shed from the blade. This sheet is made up of trailing vortex filaments associated with the blade radial distribution of lift and shed or starting vortex filaments. In transition flight the dynamic-pressure variations with azimuth angle are moderate; further, the time variations of lift and the starting or shed vortex strength are small compared with those in high-speed forward flight. However, the trailing vortices associated with the spanwise lift variations exist even for hovering. The trailing vortex sheet is unstable and rolls up into a tube which extends downstream somewhat inboard of the rotor-blade tip vortex. This rolling up process is quite complex, and more detail can be obtained from references 3 and 4. The rolled up vortex produces an upflow and downflow tendency on each side of the vortex core. The magnitude of this tendency decreases with distance from the vortex-core center. Examination of the theory of reference 5 indicates that the extent of the region as well as the direction of flow is compatible with that required to explain the measured jumps in figure 4. An example of predicted direction of flow (with the vortex center assumed to correspond to the intersection of the following blade with the tip path of the preceding blade) is included in figure 6, where it is seen that the upflow tendency region is restricted to the outer part of the blade (i.e., $r/R > 0.75$). This result is in general accord with the pressure measurements for the corresponding flight condition and lends confirmation to the premise that the jumps are caused by striking vortices from the preceding blade tip vortex.

As can be seen from figure 4, the measured jumps are a little more widely spaced in azimuth than are the tip-path intersections denoted by the ticks. These differences correspond to an inward movement, that is, the intersection of the path at $r/R = 0.90$ or 0.95 of the leading blade and the pressure-gage stations of the following blade. To determine whether this shift is compatible with predicted vortex displacement due to roll-up, it is first necessary to ascertain the time available for roll-up. This time is shown in figure 7 to correspond to an angular blade azimuth rotation of approximately 90°, or a time of $90^{\circ}/\Omega$. Based on available information such as that of reference 4, this amount of time would move the trailing vortex inboard to approximately $r/R = 0.90$ to 0.95. Since this is the amount of shift involved, it is concluded that the differences between the predicted jumps indicated by the ticks and the measured jumps in figure 4 are thus accounted for.

Thus far, the position and flow directions of the tip vortex, as a source for the jumps, have been examined. In order to determine whether the magnitude of the effect is reasonable, the measured values of the chord section loading (fig. 4) are replotted in coefficient form in figure 8. The jumps are seen to correspond to normal-force-coefficient changes of about 0.1 to 0.3, which would mean about a 1° to 3° sudden angle-of-attack change. Examination of information on vortices indicates that such magnitudes are entirely plausible. Specific prediction of magnitude of the jumps is considered too complex for the present paper. It would involve numerous factors including the spanwise lift distribution, the dynamic pressures at the times of shedding and striking the tip vortices, and the available roll-up time.

Chordwise pressure distribution.- As a check of the applicability of two-dimensional airfoil data, a comparison was made of the calculated and measured

chordwise pressure distributions in figure 9. The pressures were nondimensionalized by dividing by the calculated dynamic pressure. Azimuth angles and blade radii were chosen to be on both sides of the jumps.

One of the calculated curves (short dashed line) was obtained by choosing two-dimensional data with the same area $\left(\int_0^{1.0} \frac{-\Delta p}{q} d\left(\frac{x}{c}\right)\right)$ as the measured data and a Mach number determined from uniform inflow theory. This curve shows good agreement with the flight measured results; this agreement indicates that at a given normal-force coefficient, the chordwise pressure distribution is the same on the actual rotor as in the two-dimensional tests. Thus, the influence of unsteady effects and radial flow along the blade can be neglected and the use of two-dimensional airfoil data is justified, at least for the cases considered in figure 9.

The other calculated curve (solid line) was obtained from the angle of attack and Mach number determined from elementary (uniform) inflow theory and the corresponding chordwise pressures presented in reference 1. There are large differences between measured and calculated pressures such as would correspond to different angles of attack. These results indicate that the primary difference between blade loading on each side of the jump is caused by an unknown angle of attack due to unknown inflow velocities such as those that would be caused by trailing vortices of previous blades.

Blade bending and flapping.- There has been some disagreement as to the influence of higher harmonic blade flapping and flapwise bending on the blade load; in particular, this effect is believed to be dependent upon the specific case (e.g., proximity to resonance). For the test helicopter, the blade flap bending deflection was determined from measured bending moments and physical blade properties. The resulting velocities due to blade bending and blade flapping were combined with elementary inflow to determine a new blade airload. A comparison of the theoretical airloads with and without blade flapwise bending and higher harmonic flapping motion indicated only small differences especially when compared to the trailing vortex influence on the blade loading.

In order to determine the influence of the jump loading on blade bending moment, a dynamic analysis of the blade was made by using the theory in reference 6. In this analysis a step loading was put on the blade at three spanwise stations ($r/R = 0.75$, 0.85, and 0.95) only and at the azimuth positions indicated by the measured jumps; all other loading was made zero. A comparison was then made of the calculated and measured bending moments. The resulting comparison indicated that all bending-moment harmonics above the fourth ($4/\Omega$ through $10/\Omega$) showed good agreement.

Stalled Blade Section ($\mu = 0.23$)

This flight condition was accomplished by operating at a forward speed of 81 knots in level flight at a minimum acceptable rotor rotational speed. This condition was considered because it represents a rather extreme flight condition.

Figures 10, 11, and 12 were obtained in a manner similar to figures 6, 7, and 8 for the previous flight condition. From figure 10, it is seen that two jumps now occur on the retreating side of the blade rotation. The fact that two jumps are obtained can be explained by accounting for the trailing vortex of two leading blades (one 90° ahead of and the other 180° ahead of the instrumented blade). The short dashed part of the curve in figure 11 indicates an overlapping of trailing vortices and vortices beyond the length of the instrumented blade (i.e., $r/R > 1.0$). It is included for completeness but is of little importance for the present discussion because the vortex will have moved farther down beneath the rotor than the other vortices.

Two-Blade Rotor

A tip-path plot was made, as previously described, for the two-blade-rotor tunnel data presented in reference 7. A comparison of the predicted and measured azimuth positions of the jumps in blade loading was good as depicted in figure 13.

Other Flight Conditions

Figure 14 presents portions of the oscillograph records of the pressure transducer gages of the test helicopter. The individual gages were recorded at different gain settings; therefore, the ordinate scale for the curves is only relative and cannot be compared absolutely. The first two sets of curves are plots of the flight conditions discussed previously in this report. It will be noted that the jumps are detectable for the individual orifices. Also, increasing forward speed (V = 110 knots) decreases the magnitude of the trailing vortex influence. This is believed to be (in part at least) a result of the increased inflow velocity which causes a more rapid movement of the tip vortex away from the blade-tip-path plane.

CONCLUSIONS

Within the scope of the flight conditions (four-blade rotor at tip-speed ratios of 0.18 and 0.23) considered herein, the following qualitative conclusions are offered:

1. Large jumps found in plots of blade section loading as a function of azimuth angle are shown to occur near the intersection of the blade with the path of the preceding blade tip. Thus, the vibratory blade loading is shown to be significantly influenced by the trailing vortex of the preceding blades. This influence produces harmonic blade loadings of all orders, and the percentage of the contribution to the higher harmonics is large.

2. The influence of the blade higher harmonic flapping and flapwise bending on the higher harmonic blade loading is smaller than that of the trailing vortex.

3. The trailing-vortex tendency to produce upflow in the free-air region (forward blade azimuth position) is restricted to the outermost blade stations.

4. The blade-trailing-vortex influence decreases with an increase in forward speed.

5. The trailing-vortex influence is also present with a two-blade rotor and numerous additional flight conditions of the four-blade rotor.

Langley Research Center,
National Aeronautics and Space Administration,
Langley Station, Hampton, Va., February 6, 1963.

APPENDIX

REDUCED FLIGHT TEST DATA

Symbols

a slope of curve of section lift coefficient against section angle of attack (assumed equal to 5.73), per radian

$a_{n,s}$, $b_{n,s}$ coefficients for harmonic series of blade flapping, deg

$$\beta_s = a_0 + \sum_{n=1}^{10} (a_{n,s} \cos n\psi + b_{n,s} \sin n\psi)$$

$A_{n,s}$, $B_{n,s}$ coefficients for harmonic series of blade pitching, deg

$$\theta_s = A_0 + \sum_{n=1}^{10} (A_{n,s} \cos n\psi + B_{n,s} \sin n\psi)$$

b number of blades

E_n, F_n coefficients for harmonic series of blade lagging motion, deg

$$\zeta = E_0 + \sum_{n=1}^{10} \left(E_n \cos n\psi + F_n \sin n\psi\right)$$

I_1 mass moment of inertia of blade about flapping hinge, slug-ft^2

l section aerodynamic loading, chordwise integral of chord pressure gages, lb/in. span

L_n, M_n coefficients for harmonic series of section aerodynamic loading, lb/in. span

$$l = L_0 + \sum_{n=1}^{10} \left(L_n \cos n\psi + M_n \sin n\psi\right)$$

N_R rotor shaft rotational speed, rpm

n harmonic order

α_s angle of top of rotor shaft with respect to vertical, positive rearward and positive toward left side, deg

β_s blade flapping motion measured at blade root relative to plane normal to shaft, deg

γ mass constant of rotor blade, $c\rho aR^4/I_1$

ζ blade lag angle measured at blade root relative to rotor hub, deg

θ_s blade pitch motion measured at blade root relative to plane normal to shaft, deg

ρ mass density, slugs/cu ft

σ rotor solidity, $bc/\pi R$

Discussion

For completeness and to provide data for further analysis the reduced data for the conditions most pertinent to this paper are provided herein. The flight conditions corresponding to the three data tables are as follows:

Table	μ	V, knots	ρ, lb-sec^2/ft^4	N_R, rpm	α_s, deg	
					Long	Lateral
III	0.18	70	0.00216	226	-2.5	-0.4
IV	.23	81	.00225	193	-4.3	-.8
V	.11	41	.00250	213	-.6	-1.7

An attempt was made to evaluate the accuracy in reading the oscillograph records. The most obvious conclusion was that accuracy depended greatly upon the type and quality of the record. High-amplitude, high-frequency irregular records were most difficult to read. The estimated accuracy of each individual data point of the poorest records is ±5 percent with 99.7 percent confidence (99.7 percent of points have an error less than ±5 percent) and ±3 percent with 95 percent confidence (95 percent of points have an error less than ±3 percent). Since three consecutive cycles were averaged, the error of the tabulated data will be the square root of one-third times the foregoing values. The average individual chordwise pressure gages were integrated numerically by using the Gauss method of numerical

integration in reference 8. Because of the numerical representation of the pressure distribution and the steep gradients in pressure at the leading edge of the blade, the error in integrating the pressures chordwise is estimated to be from 0 to plus 5 percent.

The differential pressure (tables III(a), IV(a), and V(a)) represents the difference in pressure between the upper and lower surfaces at a specified blade location. A positive value represents a net negative pressure or a positive lift force.

The section aerodynamic loadings present the chordwise integral of the differential pressures. Positive values indicate positive lift per inch of span. The individual data points are presented in tables III(b), IV(b), and V(b).

All blade motions are measured at the blade root with respect to the rotor hub. The harmonic analysis of the blade motions presented in tables III(c), IV(c), and V(c) is in units of degrees where a positive sign indicates blade nose up for pitch motion, blade span axis above the plane perpendicular to the axis of the rotor shaft for flap motion, blade span axis aft of a line through the center of rotation and lag hinge for lag motion.

Tables III(d), IV(d), and V(d) present the harmonic analysis of the section aerodynamic loading given in tables III(b), IV(b), and V(b).

The blade flapwise bending moment is shown in tables III(e), IV(e), and V(e), the chordwise bending moment in tables III(f), IV(f), and V(f), and the torsional moment in tables III(g), IV(g), and V(g). In the tables, a positive sign indicates compression in the upper surface of the blade for flapwise bending moment, compression in the trailing edge of the blade for chordwise bending moment, and couple tending to rotate blade nose up for torsional moment. A positive pitch horn load indicates a down load on the end of the pitch horn.

REFERENCES

1. Lizak, Alfred A.: Two-Dimensional Wind Tunnel Tests of an H-34 Main Rotor Airfoil Section. TREC Tech. Rep. 60-53 (SER-58304), U.S. Army Transportation Res. Command (Fort Eustis, Va.), Sept. 1960.

2. Patterson, John L.: A Miniature Electrical Pressure Gage Utilizing a Stretched Flat Diaphragm. NACA TN 2659, 1952.

3. Cone, Clarence D., Jr.: A Theoretical Investigation of Vortex-Sheet Deformation Behind a Highly Loaded Wing and Its Effect on Lift. NASA TN D-657, 1961.

4. Kaden, H.: Aufwicklung einer unstabilen Unstetigkeitsfläche. Ing.-Archiv, Bd. II, Heft 2, May 1931, pp. 140-168.

5. Heyson, Harry H., and Katzoff, S.: Induced Velocities Near a Lifting Rotor With Nonuniform Disk Loading. NACA Rep. 1319, 1957. (Supersedes NACA TN 3690 by Heyson and Katzoff and TN 3691 by Heyson.)

6. Mayo, Alton P.: Matrix Method for Obtaining Spanwise Moments and Deflections of Torsionally Rigid Rotor Blades With Arbitrary Loadings. NACA TN 4304, 1958.

7. Mayo, Alton P.: Comparison of Measured Flapwise Structural Bending Moments on a Teetering Rotor Blade With Results Calculated From the Measured Pressure Distribution. NASA MEMO 2-28-59L, 1959.

8. Milne, William Edmund: Numerical Calculus. Princeton Univ. Press, 1949.

TABLE I.- PRINCIPAL DIMENSIONS AND APPROXIMATE PHYSICAL CHARACTERISTICS

OF TEST HELICOPTER AND ROTOR

Test weight, lb	11,805
Number of blades	4
Rotor-blade radius, ft	28
Flapping-hinge offset, ft	1
Weight per blade (approximate), lb	175
Main rotor blade:	
Type	All metal, constant chord
Twist, deg	-8
Airfoil section	Modified NACA 0012
Blade chord, ft	1.367
Rotor solidity, σ	0.0622
Approximate rotor-blade mass constant, γ	9.7
Normal rotor-blade tip speed, ft/sec	623
Normal rotor angular velocity, radians/sec	22.2
Test disk loading, lb/sq ft	4.79
Mass moment of inertia of blade about flapping hinge, slug-ft^2	1,176
Forward rotor shaft tilt, deg	3.0

TABLE II.- FLIGHT CHORDWISE PRESSURE-ORIFICE LOCATIONS

x/c at -						
r/R = 0.25	r/R = 0.40	r/R = 0.55	r/R = 0.75	r/R = 0.85	r/R = 0.90	r/R = 0.95
0.042	0.042	0.017	0.017	0.017	0.017	0.017
.158	.158	.090	.090	.040	.090	.090
.300	.300	.168	.168	.090	.168	.168
.600	.600	.233	.233	.130	.233	.233
.910	.910	.335	.335	.168	.335	.335
		.625	.625	.233	.625	.625
		.915	.915	.335	.915	.915
				.500		
				.625		
				.769		
				.915		

TABLE III.- REDUCED FLIGHT TEST DATA FOR $\mu = 0.18$

(a) Differential pressures

ψ_{nom}, deg	Δp, lb/sq in., at -												ψ_{nom}, deg
	r/R = 0.95							r/R = 0.90					
	x/c=.017	x/c=.090	x/c=.168	x/c=.233	x/c=.335	x/c=.625	x/c=.915	x/c=.017	x/c=.090	x/c=.168	x/c=.233	x/c=.335	
6	6.802	4.753	3.513	2.175	1.147	.520	.080	7.715	3.981	2.858	2.455	1.741	6
21	5.077	4.165	3.246	1.903	.840	.405	.036	6.244	3.361	2.453	2.232	1.483	21
36	3.984	3.705	3.079	1.704	.626	.336	.008	5.131	2.827	2.160	2.030	1.315	36
51	3.409	3.517	3.059	1.659	.489	.307	-.006	4.464	2.460	2.055	1.937	1.197	51
66	2.937	3.338	2.989	1.615	.387	.268	-.014	3.970	2.126	1.920	1.834	1.097	66
81	1.787	2.639	2.611	1.358	.217	.186	-.035	3.631	1.966	1.785	1.697	1.013	81
96	5.143	5.238	3.884	2.243	.793	.344	-.004	3.157	2.013	1.965	1.948	1.205	96
111	3.654	4.224	3.485	2.023	.721	.383	.027	5.896	3.260	2.880	2.450	1.507	111
126	3.097	3.432	2.941	1.636	.592	.349	.025	4.696	2.773	2.340	2.052	1.299	126
141	2.730	2.818	2.348	1.374	.496	.332	.027	4.289	2.387	2.055	1.730	1.181	141
156	2.692	2.682	2.115	1.306	.530	.353	.051	4.396	2.393	1.988	1.681	1.152	156
171	3.409	2.929	2.199	1.421	.663	.417	.078	4.899	2.673	2.160	1.768	1.284	171
186	3.861	3.142	2.258	1.515	.789	.443	.090	5.538	2.880	2.250	1.839	1.352	186
201	4.361	3.253	2.299	1.581	.868	.465	.097	5.789	2.967	2.318	1.844	1.376	201
216	4.625	3.338	2.313	1.615	.922	.494	.103	6.041	3.100	2.325	1.855	1.391	216
231	5.039	3.398	2.348	1.664	.994	.508	.117	6.447	3.300	2.415	1.937	1.478	231
246	5.577	3.577	2.428	1.738	1.058	.525	.125	7.009	3.534	2.505	2.024	1.546	246
261	6.397	3.892	2.649	1.897	1.191	.580	.140	8.528	3.894	2.730	2.166	1.686	261
276	7.462	4.284	2.861	2.073	1.324	.618	.146	7.938	3.501	2.475	1.986	1.586	276
291	5.200	3.227	2.223	1.510	.898	.421	.082	5.857	2.940	2.093	1.714	1.323	291
306	5.595	3.517	2.428	1.670	.987	.481	.100	6.312	3.187	2.273	1.877	1.446	306
321	6.849	4.207	2.854	1.976	1.191	.572	.119	7.560	3.761	2.678	2.232	1.670	321
336	7.961	4.863	3.294	2.298	1.375	.636	.137	8.983	4.381	3.105	2.548	1.896	336
351	8.141	5.187	3.641	2.418	1.406	.623	.121	9.486	4.581	3.255	2.733	1.972	351

ψ_{nom}, deg	Δp, lb/sq in., at -												ψ_{nom}, deg
	r/R = 0.90		r/R = 0.85										
	x/c=.625	x/c=.915	x/c=.017	x/c=.040	x/c=.090	x/c=.130	x/c=.168	x/c=.233	x/c=.335	x/c=.500	x/c=.625	x/c=.769	
6	.635	.042	8.724	5.804	4.263	3.212	2.703	2.296	1.500	.735	.636	.316	6
21	.515	-.019	6.845	5.190	3.733	2.775	2.403	1.947	1.292	.564	.522	.228	21
36	.425	-.068	5.810	4.499	3.402	2.422	2.151	1.721	1.133	.435	.430	.175	36
51	.356	-.115	5.199	4.049	3.192	2.310	2.003	1.564	1.043	.349	.363	.122	51
66	.295	-.153	4.529	3.589	2.932	2.140	1.847	1.362	.926	.242	.290	.079	66
81	.228	-.169	4.267	3.314	2.771	1.844	1.735	1.235	.831	.167	.228	.049	81
96	.379	-.145	4.325	3.413	2.841	1.981	1.743	1.324	.911	.237	.300	.100	96
111	.467	-.115	4.762	3.907	3.302	2.422	2.091	1.663	1.179	.420	.445	.206	111
126	.443	-.096	6.306	5.135	4.063	2.916	2.459	1.865	1.277	.448	.465	.214	126
141	.430	-.077	5.301	4.071	3.272	2.375	2.035	1.557	1.106	.399	.455	.217	141
156	.443	-.038	5.242	4.005	3.152	2.291	1.975	1.509	1.077	.428	.487	.252	156
171	.500	-.007	5.621	4.225	3.252	2.408	2.083	1.612	1.153	.506	.533	.303	171
186	.448	.063	6.131	4.532	3.412	2.559	2.183	1.732	1.236	.576	.579	.337	186
201	.579	.082	6.364	4.597	3.402	2.573	2.175	1.783	1.247	.608	.600	.351	201
216	.589	.108	6.495	4.586	3.402	2.587	2.171	1.800	1.251	.644	.610	.358	216
231	.622	.120	7.019	4.773	3.552	2.733	2.263	1.910	1.310	.702	.642	.375	231
246	.659	.129	7.617	5.036	3.733	2.897	2.371	2.023	1.369	.759	.663	.390	246
261	.715	.145	8.651	5.321	3.913	3.029	2.523	2.139	1.447	.813	.688	.396	261
276	.659	.127	5.665	3.808	2.851	2.173	1.791	1.564	1.038	.571	.518	.281	276
291	.551	.090	5.825	3.896	2.942	2.216	1.815	1.609	1.024	.560	.502	.276	291
306	.607	.099	6.175	4.181	3.112	2.361	1.951	1.701	1.111	.608	.543	.292	306
321	.697	.113	7.500	5.058	3.763	2.874	2.367	2.043	1.327	.738	.632	.343	321
336	.753	.118	9.394	5.924	4.424	3.409	2.811	2.396	1.599	.876	.724	.393	336
351	.766	.096	9.874	6.067	4.694	3.565	2.983	2.488	1.670	.876	.730	.375	351

TABLE III.- REDUCED FLIGHT TEST DATA FOR μ = 0.18 - Continued

(a) Differential pressures - Concluded

ψ_{nom}, deg	Δp, lb/sq in., at -												ψ_{nom}, deg
	r/R = 0.85	r/R = 0.75							r/R = 0.55				
	x/c=.915	x/c=.017	x/c=.090	x/c=.168	x/c=.233	x/c=.335	x/c=.625	x/c=.915	x/c=.017	x/c=.090	x/c=.168	x/c=.233	
6	.078	6.550	3.391	2.449	1.969	1.303	.528	.031	3.464	1.645	1.142	1.009	6
21	.029	6.135	3.043	2.250	1.834	1.174	.461	.015	3.439	1.639	1.153	.995	21
36	-.006	5.562	2.834	2.199	1.749	1.080	.418	.010	3.413	1.639	1.136	.984	36
51	-.052	4.988	2.629	2.127	1.692	.998	.372	-.040	3.266	1.586	1.092	.954	51
66	-.059	4.377	2.395	1.995	1.559	.879	.313	-.023	3.016	1.453	1.015	.890	66
81	-.084	3.781	2.141	1.829	1.431	.742	.260	-.007	2.907	1.412	.958	.840	81
96	-.069	3.503	2.092	1.856	1.446	.761	.292	.010	3.202	1.564	1.079	.934	96
111	-.037	4.071	2.550	2.211	1.731	.947	.368	.024	3.829	1.881	1.299	1.106	111
126	-.011	4.344	2.649	2.307	1.825	1.074	.415	.050	3.887	1.902	1.356	1.167	126
141	-.024	4.497	2.619	2.268	1.812	1.129	.435	.067	4.143	2.023	1.431	1.244	141
156	.018	5.256	3.092	2.455	1.904	1.211	.465	.086	4.034	1.961	1.379	1.194	156
171	.033	5.502	3.038	2.389	1.853	1.229	.503	.096	3.740	1.846	1.325	1.151	171
186	.061	5.682	3.112	2.365	1.836	1.229	.508	.088	3.586	1.716	1.212	1.063	186
201	.070	5.775	3.038	2.268	1.766	1.206	.498	.077	3.074	1.456	1.044	.924	201
216	.085	5.698	2.983	2.178	1.712	1.170	.500	.086	2.747	1.282	.922	.830	216
231	.105	5.824	3.073	2.193	1.725	1.206	.526	.084	2.466	1.121	.811	.739	231
246	.108	5.977	3.247	2.259	1.771	1.243	.535	.086	2.133	.972	.704	.650	246
261	.133	5.469	2.191	1.616	1.237	.865	.348	.003	1.896	.860	.635	.585	261
276	.055	4.775	2.206	1.567	1.235	.855	.375	.026	1.704	.761	.570	.539	276
291	.085	4.333	2.166	1.543	1.217	.838	.361	.024	1.601	.727	.531	.503	291
306	.097	4.142	2.181	1.558	1.246	.851	.380	.022	1.819	.814	.589	.547	306
321	.118	4.530	2.604	1.844	1.494	1.039	.461	.041	2.344	1.080	.765	.689	321
336	.080	5.316	3.192	2.244	1.823	1.280	.561	.053	3.010	1.409	.981	.866	336
351	.085	6.206	3.546	2.521	2.023	1.399	.583	.043	3.432	1.623	1.121	1.000	351

ψ_{nom}, deg	Δp, lb/sq in., at -													ψ_{nom}, deg
	r/R = 0.55			r/R = 0.40					r/R = 0.25					
	x/c=.335	x/c=.625	x/c=.915	x/c=.042	x/c=.158	x/c=.300	x/c=.600	x/c=.910	x/c=.042	x/c=.158	x/c=.300	x/c=.600	x/c=.910	
6	.784	.404	.080	1.162	.633	.386	.296	.081	.422	.192	.120	.085	.022	6
21	.784	.404	.089	1.436	.747	.461	.330	.090	.698	.322	.193	.116	.033	21
36	.777	.410	.101	1.423	.737	.461	.323	.096	.661	.305	.183	.111	.031	36
51	.765	.392	.101	1.512	.773	.489	.335	.100	.766	.356	.212	.116	.036	51
66	.717	.379	.102	1.490	.794	.489	.333	.100	.826	.390	.231	.122	.041	66
81	.692	.365	.104	1.479	.788	.491	.343	.106	.923	.432	.259	.131	.047	81
96	.738	.386	.115	1.525	.815	.509	.368	.115	1.020	.499	.296	.152	.056	96
111	.869	.449	.128	1.883	1.031	.642	.436	.130	1.190	.583	.365	.172	.065	111
126	.924	.470	.130	2.120	1.148	.699	.469	.139	1.174	.641	.422	.206	.074	126
141	.987	.479	.130	2.120	1.148	.701	.461	.126	1.589	.771	.467	.213	.075	141
156	.952	.465	.132	1.956	1.095	.677	.458	.117	1.377	.717	.443	.204	.071	156
171	.924	.446	.100	2.085	1.129	.665	.419	.100	1.214	.623	.393	.195	.066	171
186	.840	.404	.080	1.695	.982	.587	.390	.095	1.046	.515	.327	.166	.056	186
201	.729	.358	.061	1.418	.822	.484	.336	.075	.701	.331	.207	.113	.036	201
216	.654	.316	.045	1.103	.648	.379	.273	.059	.435	.181	.109	.071	.021	216
231	.574	.280	.025	.834	.499	.283	.218	.042	.255	.084	.043	.035	.007	231
246	.516	.259	.014	.599	.379	.208	.175	.027	.152	.034	.009	.026	.005	246
261	.474	.229	.006	.457	.307	.167	.156	.027	.101	.005	-.009	.017	.004	261
276	.433	.216	-.002	.333	.245	.129	.142	.027	.092	.000	-.012	.017	-.002	276
291	.402	.195	-.002	.303	.228	.120	.143	.023	.097	.007	-.003	.025	.001	291
306	.425	.216	.010	.355	.241	.136	.153	.034	.111	.023	.008	.034	.005	306
321	.530	.286	.037	.457	.296	.181	.184	.044	.090	.019	.012	.044	.012	321
336	.663	.356	.059	.702	.415	.260	.234	.061	.032	-.005	.003	.033	.004	336
351	.772	.392	.077	1.003	.565	.349	.274	.073	.037	.008	.018	.049	.007	351

TABLE III.- REDUCED FLIGHT TEST DATA FOR μ = 0.18 - Continued

(b) Section aerodynamic loading

ψ_{nom}, deg	Section aerodynamic loading, l, lb/in., at -						
	r/R = 0.25	r/R = 0.40	r/R = 0.55	r/R = 0.75	r/R = 0.85	r/R = 0.90	r/R = 0.95
6	2.019	6.367	12.129	21.435	26.176	26.086	24.619
21	3.171	7.507	12.139	19.442	21.953	21.741	20.203
36	3.010	7.451	12.139	18.045	19.095	18.449	17.225
51	3.418	7.842	11.741	16.516	17.229	16.326	15.825
66	3.695	7.829	11.001	14.816	15.219	14.460	14.529
81	4.099	7.888	10.600	13.027	13.823	13.013	10.966
96	4.658	8.252	11.557	13.105	14.751	14.719	22.167
111	5.475	10.128	13.691	15.911	18.215	21.578	19.107
126	5.982	11.141	14.190	17.217	21.525	18.268	15.996
141	7.084	11.054	14.958	17.580	18.261	16.431	13.506
156	6.493	10.561	14.501	19.590	18.161	16.496	13.246
171	5.819	10.496	13.722	19.872	19.350	18.397	15.186
186	4.921	9.144	12.637	20.057	20.784	19.496	16.559
201	3.235	7.665	10.897	19.673	21.148	20.751	17.585
216	1.897	6.056	9.655	19.303	21.369	21.323	18.297
231	.942	4.639	8.483	19.802	22.596	22.583	19.128
246	.507	3.478	7.484	20.451	23.824	23.952	20.257
261	.255	2.868	6.689	14.820	25.588	26.775	22.489
276	.199	2.343	6.058	14.464	18.016	24.640	24.879
291	.309	2.224	5.639	13.905	18.286	20.061	17.813
306	.465	2.487	6.258	13.969	19.578	21.837	19.572
321	.522	3.125	8.166	16.530	23.511	25.614	23.456
336	.262	4.363	10.418	20.073	27.919	29.370	27.003
351	.450	5.703	11.925	22.200	29.218	30.593	28.102

(c) Harmonic analysis of blade root motions

Pitch motion			Flap motion			Lag motion		
n	$A_{n,s}$, deg	$B_{n,s}$, deg	n	$a_{n,s}$, deg	$b_{n,s}$, deg	n	E_n, deg	F_n, deg
0	13.6860	--	0	3.9331	--	0	5.9872	--
1	.6950	-4.8005	1	.5508	-.5794	1	-.1296	.0486
2	-.0263	.0526	2	0	.0367	2	-.0176	.0270
3	.0818	.0847	3	.0653	-.0490	3	.0189	-.0148
4	0	-.0380	4	.0530	-.0041	4	.0054	-.0148
5	-.0350	-.0117	5	-.0408	0	5	.0054	.0014
6	.0058	.0204	6	-.0041	0	6	.0027	.0148
7	-.0088	.0117	7	-.0122	.0163	7	-.0027	.0068
8	.0029	0	8	.0204	.0122	8	-.0094	.0027
9	.0204	-.0058	9	.0653	-.0041	9	0	-.0027
10	.0175	.0058	10	-.0041	-.0082	10	.0040	-.0014
$\theta_s = A_o + \sum_{n=1}^{n}\left[A_{n,s}\cos n\left(\psi_{nom} - 6^\circ\right) + B_{n,s}\sin n\left(\psi_{nom} - 6^\circ\right)\right]$			$\beta_s = a_o + \sum_{n=1}^{n}\left[a_{n,s}\cos n\left(\psi_{nom} - 6^\circ\right) + b_{n,s}\sin n\left(\psi_{nom} - 6^\circ\right)\right]$			$\zeta = E_o + \sum_{n=1}^{n}\left[E_n\cos n(\psi_{nom} - 6^\circ) + F_n\sin n(\psi_{nom} - 6^\circ)\right]$		

TABLE III.- REDUCED FLIGHT TEST DATA FOR $\mu = 0.18$ - Continued

(d) Harmonic analysis of section aerodynamic loading

r/R	n	L_n, lb/in.	M_n, lb/in.	r/R	n	L_n, lb/in.	M_n, lb/in.	r/R	n	L_n, lb/in.	M_n, lb/in.
.25	0	2.8702		.75	0	17.5751		.95	0	19.0714	
.25	1	-1.4148	2.6780	.75	1	-.4798	-.5278	.95	1	2.8630	-3.3416
.25	2	.3988	-.6197	.75	2	3.2978	.1062	.95	2	.5089	-.9385
.25	3	-.0492	.5546	.75	3	1.4580	-.3269	.95	3	2.1299	-1.7947
.25	4	.0068	.1418	.75	4	-.3061	-.5331	.95	4	1.5810	-.4318
.25	5	.0476	.1381	.75	5	-.2044	-.0831	.95	5	-1.4217	-.4410
.25	6	.0891	.1627	.75	6	.2804	-.5945	.95	6	-.9404	-.5796
.25	7	.0132	.0393	.75	7	-.1942	-.0560	.95	7	.7548	-.0961
.25	8	.1000	.0845	.75	8	-.1390	.3905	.95	8	.9459	.1379
.25	9	-.0462	.0738	.75	9	.2521	-.2632	.95	9	-.4279	.2247
.25	10	.0327	-.0290	.75	10	-.0974	-.1487	.95	10	-1.0355	-.1433
.40	0	6.6921		.85	0	20.6497					
.40	1	-1.4965	3.5435	.85	1	1.1497	-3.0276				
.40	2	1.1516	-.5205	.85	2	2.5864	-.8227				
.40	3	.2838	.3078	.85	3	2.6535	-1.1927				
.40	4	.0002	.1064	.85	4	-.1187	-.8616				
.40	5	-.1245	-.1338	.85	5	-1.2346	-.6520				
.40	6	.1183	-.0770	.85	6	.6495	-.0508				
.40	7	-.0036	.1255	.85	7	.1737	-.0662				
.40	8	-.0963	-.0242	.85	8	-.4842	-.3481				
.40	9	-.0295	.0271	.85	9	.0038	.2683				
.40	10	-.0409	.0189	.85	10	.3122	.2851				
.55	0	10.6948		.90	0	20.9566					
.55	1	-.6839	3.1787	.90	1	1.9283	-4.5625				
.55	2	1.7907	-.8026	.90	2	1.5409	-1.1711				
.55	3	.7451	.1553	.90	3	2.5476	-1.3341				
.55	4	-.0949	-.1251	.90	4	.6970	-.6533				
.55	5	-.2479	-.1839	.90	5	-1.5371	-.7966				
.55	6	-.0524	-.1460	.90	6	-.0748	-.4344				
.55	7	.0261	.0047	.90	7	.6985	.2840				
.55	8	.0212	.0427	.90	8	-.2197	-.0178				
.55	9	-.0939	-.0226	.90	9	-.4621	-.3629				
.55	10	.0494	-.0683	.90	10	.0896	-.0472				

$$l = L_0 + \sum_{n=1}^{n} \left[L_n \cos n\left(\psi_{nom} - 6^\circ\right) + M_n \sin n\left(\psi_{nom} - 6^\circ\right) \right]$$

TABLE III.- REDUCED FLIGHT TEST DATA FOR μ = 0.18 - Concluded

(e) Flapwise bending moment

ψ_{nom}, deg	Flapwise bending moment, in-lb, at -							
	r/R = 0.150	r/R = 0.275	r/R = 0.375	r/R = 0.450	r/R = 0.575	r/R = 0.650	r/R = 0.800	r/R = 0.925
6	1808	1535	1519	-36	-1707	-4286	-6721	-5818
21	2868	2038	1935	737	-1056	-4116	-5805	-4285
36	1682	1823	2269	1138	-343	-2505	-3823	-3614
51	1260	1064	1329	403	71	-1500	-2144	-2613
66	1443	462	597	-198	-915	-2664	-2218	-2037
81	1203	421	127	-1400	-2420	-4196	-4974	-3679
96	850	-347	-606	-1972	-3748	-6544	-5392	-3212
111	725	-850	-1926	-3442	-3572	-5062	-4419	-4190
126	-244	-1287	-1374	-2239	-2552	-4405	-5528	-4132
141	1067	-157	154	-904	-2569	-5470	-6517	-3665
156	2720	1262	696	-1266	-2868	-5400	-6804	-4373
171	1397	363	570	-799	-2358	-5360	-6187	-3811
186	896	-553	-470	-1228	-1504	-4296	-5957	-4234
201	975	347	127	-1352	-2332	-4753	-4906	-3665
216	2674	1271	814	-465	-1689	-4793	-6501	-4387
231	2058	2195	2649	1433	-580	-3669	-7254	-5205
246	2560	2475	2992	2149	1250	-604	-5010	-4709
261	2207	2269	3037	2693	2834	2023	256	-3088
276	1112	2401	3697	3494	3793	3465	3185	-1205
291	1796	2830	3960	3723	3864	3137	1543	-1453
306	2252	2879	4023	3609	2605	321	-2343	-3504
321	1716	2624	3218	1853	194	-2037	-4676	-5227
336	1511	1172	1148	327	-915	-3480	-5376	-5285
351	371	759	886	-236	-1592	-4116	-6098	-5884

(f) Chordwise bending moment

ψ_{nom}, deg	Chordwise bending moment, in-lb, at -			
	r/R = 0.150	r/R = 0.375	r/R = 0.575	r/R = 0.825
6	-6741	-7700	1451	14393
21	-7767	-7489	1643	14036
36	-5113	-5307	2571	14064
51	-4446	-2393	6203	15445
66	-2573	-602	7003	15518
81	-1092	-309	5627	14631
96	-1206	-2051	5051	14576
111	259	-2149	3003	13469
126	1513	-2702	2971	14118
141	-34	-1563	5099	14933
156	-490	33	7403	16003
171	569	2214	8683	15875
186	178	2230	8987	16360
201	-717	-521	7307	16433
216	-1759	-2572	3675	14539
231	-5032	-6561	2715	15390
246	-6936	-7961	1387	14686
261	-6904	-7310	27	13139
276	-10030	-8921	1899	14603
291	-12065	-8270	2587	14713
306	-10551	-7179	3131	14732
321	-9753	-5421	4443	15464
336	-7750	-5161	4315	15601
351	-5113	-5568	1883	13853

(g) Blade torsional moment and pitch horn load

ψ_{nom}, deg	Torsional moment, in-lb, at -		Pitch horn load, lb
	r/R = 0.15	r/R = 0.50	
6	503	485	157
21	397	494	139
36	464	507	153
51	591	556	166
66	569	723	150
81	389	503	128
96	382	510	96
111	455	513	80
126	368	345	38
141	-156	-80	2
156	-422	-382	-17
171	-505	-324	-27
186	-544	-365	-29
201	-479	-411	-39
216	-412	-469	-14
231	-191	-364	1
246	-304	-423	11
261	-202	-229	26
276	-251	-289	43
291	-609	-448	50
306	-780	-515	35
321	-448	-219	68
336	147	215	129
351	556	719	157

TABLE IV.- REDUCED FLIGHT TEST DATA FOR $\mu = 0.23$

(a) Differential pressures

ψ_{nom}, deg	Δp, lb/sq in., at -												ψ_{nom}, deg
	r/R = 0.95							r/R = 0.90					
	x/c=.017	x/c=.090	x/c=.168	x/c=.233	x/c=.335	x/c=.625	x/c=.915	x/c=.017	x/c=.090	x/c=.168	x/c=.233	x/c=.335	
0	9.653	5.110	2.867	2.254	1.348	.618	.219	8.784	4.411	3.021	2.474	1.761	0
15	9.423	5.033	2.899	2.185	1.143	.416	.099	9.458	4.215	2.874	2.362	1.474	15
30	7.385	5.033	2.920	2.166	1.116	.543	.069	7.943	3.953	2.874	2.524	1.588	30
45	5.510	4.361	2.839	1.922	.891	.483	.042	6.107	3.422	2.550	2.294	1.385	45
60	3.950	3.681	2.336	1.589	.594	.388	.006	4.641	2.727	2.102	1.879	1.128	60
75	3.060	3.239	2.119	1.436	.418	.340	-.006	3.449	2.052	1.668	1.548	.917	75
90	1.979	2.746	1.839	1.205	.269	.309	-.022	2.560	1.653	1.397	1.430	.759	90
105	2.352	2.839	2.009	1.179	.256	.293	-.014	2.374	1.482	1.272	1.329	.713	105
120	1.749	2.252	1.683	.991	.230	.317	.022	2.531	1.633	1.301	1.397	.721	120
135	2.247	2.414	1.754	1.125	.355	.368	.026	3.029	1.928	1.492	1.537	.850	135
150	2.706	2.644	1.637	1.243	.461	.404	.049	3.420	2.144	1.610	1.599	.939	150
165	3.749	3.222	2.091	1.573	.723	.523	.093	4.377	2.609	1.926	1.834	1.166	165
180	4.955	3.817	2.378	1.790	.951	.614	.118	5.872	3.304	2.426	2.126	1.407	180
195	5.385	3.919	2.321	1.817	1.020	.626	.132	6.380	3.455	2.514	2.120	1.458	195
210	5.615	3.860	2.201	1.777	1.043	.614	.134	6.458	3.389	2.396	2.008	1.423	210
225	5.529	3.707	2.052	1.686	1.014	.590	.134	6.781	3.199	2.271	1.907	1.354	225
240	5.490	3.621	1.999	1.645	1.000	.586	.146	6.869	3.127	2.154	1.851	1.324	240
255	5.911	3.809	2.098	1.747	1.106	.606	.156	5.921	3.356	2.279	1.907	1.369	255
270	5.634	3.604	1.903	1.573	.951	.511	.119	3.869	2.917	2.102	1.806	1.301	270
285	5.720	3.647	1.985	1.637	1.014	.559	.162	3.332	2.210	1.661	1.498	1.204	285
300	5.309	3.451	1.740	1.361	.779	.527	.211	3.742	2.124	1.404	1.301	1.067	300
315	5.079	3.681	2.268	2.278	1.712	.839	.251	3.215	3.009	2.528	2.334	1.873	315
330	6.342	3.409	1.528	1.117	.766	.563	.300	4.641	2.387	1.639	1.464	1.105	330
345	8.198	4.455	2.403	1.825	.961	.436	.170	8.129	3.297	2.301	1.941	1.316	345

ψ_{nom}, deg	Δp, lb/sq in., at -												ψ_{nom}, deg
	r/R = 0.90		r/R = 0.85										
	x/c=.625	x/c=.915	x/c=.017	x/c=.040	x/c=.090	x/c=.130	x/c=.168	x/c=.233	x/c=.335	x/c=.500	x/c=.625	x/c=.769	
0	.740	.317	5.572	5.253	4.930	4.098	3.212	2.857	1.654	.951	.817	.542	0
15	.387	.193	8.981	5.705	4.045	3.123	2.397	2.097	1.069	.543	.541	.409	15
30	.570	.031	9.174	5.816	4.271	3.248	2.584	2.337	1.363	.691	.586	.303	30
45	.492	.000	7.188	5.065	3.789	2.840	2.331	2.080	1.192	.558	.551	.280	45
60	.365	-.060	5.750	4.193	3.288	2.341	1.918	1.764	.967	.364	.416	.196	60
75	.287	-.103	4.416	3.221	2.668	2.144	1.692	1.384	.744	.201	.310	.118	75
90	.231	-.124	3.468	2.349	2.137	1.664	1.256	1.131	.548	.064	.229	.085	90
105	.231	-.108	2.742	1.808	1.783	1.352	1.006	1.018	.459	.047	.199	.080	105
120	.274	-.094	4.150	2.868	2.521	1.875	1.458	1.161	.679	.189	.305	.155	120
135	.322	-.065	4.298	3.000	2.688	1.880	1.548	1.295	.821	.285	.416	.228	135
150	.379	-.025	4.787	3.332	2.884	2.144	1.680	1.439	.912	.359	.486	.274	150
165	.492	.063	5.706	3.939	3.288	2.490	1.992	1.775	1.095	.506	.606	.378	165
180	.596	.094	7.202	4.855	3.799	2.974	2.366	2.097	1.307	.642	.711	.449	180
195	.606	.105	8.047	4.943	3.868	3.037	2.405	2.158	1.326	.661	.721	.451	195
210	.592	.114	7.766	4.712	3.681	2.888	2.273	2.063	1.258	.646	.681	.425	210
225	.561	.119	7.321	4.380	3.425	2.720	2.117	1.953	1.161	.617	.631	.396	225
240	.561	.135	6.358	4.193	3.278	2.610	2.015	1.881	1.106	.614	.611	.389	240
255	.575	.159	5.083	3.972	3.534	2.874	2.241	2.107	1.198	.632	.591	.378	255
270	.492	.173	2.742	2.150	2.245	1.990	1.579	1.703	1.075	.699	.717	.555	270
285	.579	.245	2.164	1.554	1.616	1.376	.897	1.000	.636	.429	.500	.409	285
300	.496	.250	3.957	2.537	2.058	1.693	1.244	1.292	.650	.416	.531	.360	300
315	1.014	.306	3.290	3.144	3.347	3.090	2.577	2.614	1.489	.810	.687	.422	315
330	.501	.277	4.150	3.332	3.012	2.451	1.782	1.730	1.095	.649	.737	.636	330
345	.566	.261	7.855	4.954	3.661	2.806	2.086	1.970	1.072	.624	.621	.404	345

TABLE IV.- REDUCED FLIGHT TEST DATA FOR μ = 0.23 - Continued

(a) Differential pressures - Concluded

ψ_{nom}, deg	Δp, lb/sq in., at -												ψ_{nom}, deg
	r/R = 0.85	r/R = 0.75							r/R = 0.55				
	x/c=.915	x/c=.017	x/c=.090	x/c=.168	x/c=.233	x/c=.335	x/c=.625	x/c=.915	x/c=.017	x/c=.090	x/c=.168	x/c=.233	
0	.209	6.014	4.262	2.758	2.143	1.636	.690	.173	3.275	1.576	1.097	1.138	0
15	.209	7.076	3.889	2.659	1.982	1.394	.543	.095	3.603	1.588	1.061	1.093	15
30	-.005	7.330	3.715	2.519	1.969	1.375	.554	.060	3.496	1.623	1.074	1.114	30
45	-.015	6.661	3.367	2.348	1.863	1.270	.525	.058	3.325	1.510	1.023	1.070	45
60	-.066	5.799	3.029	2.187	1.709	1.109	.445	.036	2.890	1.336	.880	.958	60
75	-.111	4.737	2.482	1.824	1.460	.880	.335	.005	2.348	1.071	.668	.800	75
90	-.132	3.581	1.830	1.312	1.152	.627	.247	.015	2.033	.920	.677	.718	90
105	-.136	2.774	1.805	1.219	1.075	.595	.234	.015	1.888	.851	.628	.650	105
120	-.101	2.879	2.164	1.449	1.231	.743	.327	.053	3.035	1.494	.968	.998	120
135	-.062	4.024	2.964	2.119	1.656	1.086	.445	.086	3.401	1.658	1.139	1.167	135
150	-.052	4.825	3.094	2.321	1.790	1.199	.510	.119	3.388	1.645	1.130	1.164	150
165	-.009	5.395	3.372	2.432	1.879	1.336	.582	.131	3.565	1.740	1.206	1.212	165
180	.022	6.058	3.785	2.625	2.037	1.480	.651	.142	3.628	1.790	1.252	1.338	180
195	.033	6.534	3.710	2.519	1.942	1.441	.623	.131	3.849	1.929	1.328	1.380	195
210	.033	6.750	3.462	2.311	1.775	1.328	.567	.116	.570	.847	1.080	1.417	210
225	.034	5.987	3.183	2.091	1.601	1.199	.510	.107	.853	.472	.433	.736	225
240	.041	5.229	2.939	1.902	1.418	1.090	.463	.114	.507	.611	.649	.821	240
255	.088	4.427	2.318	1.911	1.656	1.504	.479	.102	.809	.242	.322	.692	255
270	.205	3.056	1.378	1.030	.670	.871	.543	.287	.633	.113	.107	.475	270
285	.234	2.000	1.288	.760	.564	.541	.499	.105	.778	.182	.166	.401	285
300	.033	2.674	2.283	1.396	1.066	.785	.329	.086	.992	.371	.305	.499	300
315	.149	3.537	3.019	1.852	1.403	1.071	.460	.110	1.434	.564	.424	.592	315
330	.490	4.328	3.009	2.141	1.674	1.274	.574	.176	1.490	.617	.445	.615	330
345	.122	5.019	3.248	2.048	1.568	1.128	.484	.107	2.260	1.059	.733	.826	345

ψ_{nom}, deg	Δp, lb/sq in., at -													ψ_{nom}, deg
	r/R = 0.55			r/R = 0.40					r/R = 0.25					
	x/c=.335	x/c=.625	x/c=.915	x/c=.042	x/c=.158	x/c=.300	x/c=.600	x/c=.910	x/c=.042	x/c=.158	x/c=.300	x/c=.600	x/c=.910	
0	.903	.438	.095	.740	.525	.255	.268	.093	.338	.130	.062	.132	.028	0
15	.864	.409	.067	1.150	.701	.342	.275	.092	.558	.194	.096	.134	.024	15
30	.876	.415	.080	1.416	.781	.395	.306	.101	.798	.351	.177	.155	.028	30
45	.861	.428	.094	1.552	.837	.429	.318	.106	.763	.305	.153	.153	.025	45
60	.787	.403	.094	1.436	.778	.396	.300	.105	.820	.339	.172	.148	.032	60
75	.683	.349	.087	1.245	.705	.356	.290	.105	.736	.298	.145	.147	.032	75
90	.623	.304	.081	.873	.614	.294	.270	.101	.677	.271	.131	.139	.036	90
105	.575	.298	.086	1.333	.807	.387	.325	.116	1.058	.495	.278	.194	.049	105
120	.792	.393	.114	1.488	.867	.474	.380	.134	1.107	.501	.289	.214	.059	120
135	.951	.450	.124	1.896	1.051	.604	.426	.150	1.273	.594	.342	.227	.066	135
150	.955	.463	.126	2.176	1.241	.714	.469	.143	1.383	.642	.380	.242	.069	150
165	.994	.491	.119	2.207	1.245	.705	.465	.135	1.523	.768	.455	.281	.075	165
180	1.045	.517	.114	2.060	1.161	.635	.422	.121	1.497	.711	.420	.266	.070	180
195	1.035	.444	.125	1.680	.962	.491	.350	.099	.977	.558	.284	.209	.054	195
210	1.319	.532	.120	1.147	.733	.338	.272	.081	.644	.395	.091	.138	.032	210
225	.799	.748	.379	.734	.530	.212	.204	.060	.287	.278	.006	.082	.017	225
240	.734	.421	.229	.407	.372	.115	.157	.046	.144	.082	-.032	.058	.001	240
255	.701	.345	.074	.205	.259	.039	.124	.034	.132	.020	-.052	.036	-.007	255
270	.277	.203	.026	.102	.201	.007	.113	.035	.142	-.013	-.061	.046	-.027	270
285	.318	.130	-.004	.047	.210	.014	.133	.038	.124	-.020	-.056	.056	-.041	285
300	.409	.193	.014	.108	.225	.040	.156	.061	.123	-.009	-.026	.077	-.021	300
315	.472	.219	.034	.255	.290	.086	.165	.056	.144	.012	-.007	.091	-.003	315
330	.479	.247	.037	.404	.359	.132	.170	.060	.100	-.013	-.036	.073	.006	330
345	.657	.313	.065	.518	.417	.181	.233	.083	.104	-.008	-.024	.084	.010	345

TABLE IV.- REDUCED FLIGHT TEST DATA FOR μ = 0.23 - Continued

(b) Section aerodynamic loading

ψ_{nom}, deg	Section aerodynamic loading, l, lb/in., at -						
	r/R = 0.25	r/R = 0.40	r/R = 0.55	r/R = 0.75	r/R = 0.85	r/R = 0.90	r/R = 0.95
0	1.864	4.902	12.575	25.266	27.849	29.248	28.040
15	2.450	6.217	12.360	23.387	23.971	25.863	25.552
30	3.533	7.190	12.481	23.014	25.358	25.370	24.595
45	3.290	7.717	12.173	21.234	21.942	21.505	20.866
60	3.505	7.202	10.963	18.768	17.768	16.835	16.254
75	3.196	6.565	9.143	15.111	13.901	12.953	13.712
90	2.972	5.449	8.194	11.180	10.551	10.408	10.994
105	4.867	7.233	7.703	10.203	8.652	9.701	11.493
120	5.150	8.288	11.458	12.326	12.821	10.415	9.860
135	5.869	10.058	13.182	17.362	14.593	12.330	11.348
150	6.365	11.455	13.233	19.337	16.218	13.858	12.553
165	7.323	11.427	13.887	21.237	19.513	17.460	16.625
180	6.954	10.492	14.451	23.550	23.417	21.852	20.198
195	4.965	8.519	14.535	23.258	24.373	22.802	20.937
210	3.072	6.192	11.839	21.937	23.222	22.365	20.853
225	1.495	4.251	10.467	19.808	21.667	21.714	20.089
240	.595	2.778	8.237	17.942	20.313	21.435	19.816
255	.237	1.749	6.369	18.171	20.569	21.579	21.084
270	.159	1.308	3.238	12.843	16.632	18.560	19.047
285	.143	1.385	3.100	9.533	11.361	16.796	19.947
300	.464	1.822	4.482	12.414	13.458	15.585	18.049
315	.749	2.371	5.713	16.656	21.566	24.421	24.587
330	.458	2.940	6.056	19.338	20.122	17.270	18.733
345	.596	3.851	8.809	18.731	22.283	23.265	22.694

(c) Harmonic analysis of blade root motion

Pitch motion			Flap motion			Lag motion		
n	$A_{n,s}$, deg	$B_{n,s}$, deg	n	$a_{n,s}$, deg	$b_{n,s}$, deg	n	E_n, deg	F_n, deg
0	15.1404	--	0	4.2127	--	0	9.3690	--
1	3.5014	-7.5144	1	-.8507	-.7894	1	-.6587	.2842
2	.1814	.3348	2	-.3906	-.5092	2	.0175	.0612
3	-.3302	-.0140	3	.1268	-.0818	3	.0766	-.0644
4	-.1302	-.0046	4	.0941	.0389	4	-.0175	.0094
5	-.1581	.2558	5	.0736	.0941	5	-.0016	.0345
6	.1860	.2930	6	.0102	.0634	6	.0096	0
7	.1860	.2139	7	.0164	.0164	7	0	0
8	.1581	-.0698	8	.0409	.0368	8	.0064	.0096
9	.0558	-.0930	9	.0225	.0102	9	-.0160	-.0032
10	-.0046	-.0884	10	.0245	.0061	10	-.0032	-.0016
$\theta_s = A_o + \sum_{n=1}^{n}\left(A_{n,s} \cos n\psi_{nom} + B_{n,s} \sin n\psi_{nom}\right)$			$\beta_s = a_o + \sum_{n=1}^{n}\left(a_{n,s} \cos n\psi_{nom} + b_{n,s} \sin n\psi_{nom}\right)$			$\zeta = E_o + \sum_{n=1}^{n}\left(E_n \cos n\psi_{nom} + F_n \sin n\psi_{nom}\right)$		

TABLE IV.- REDUCED FLIGHT TEST DATA FOR $\mu = 0.23$ - Continued

(d) Harmonic analysis of section aerodynamic loading

r/R	n	L_n, lb/in.	M_n, lb/in.	r/R	n	L_n, lb/in.	M_n, lb/in.	r/R	n	L_n, lb/in.	M_n, lb/in.
.25	0	2.9279		.75	0	18.0252		.95	0	18.6633	
.25	1	-1.8690	2.1646	.75	1	.0295	-.0504	.95	1	3.2715	-3.6602
.25	2	1.1259	-.3644	.75	2	5.4145	2.7447	.95	2	3.4603	2.4678
.25	3	-.5208	.4991	.75	3	.1041	.6499	.95	3	.0078	.5804
.25	4	.0719	.1710	.75	4	-.4119	-.9070	.95	4	.5878	.7086
.25	5	-.2506	.0488	.75	5	-.2906	-.1120	.95	5	-.3781	.3513
.25	6	.1644	-.0206	.75	6	.2180	1.0999	.95	6	.4535	.4588
.25	7	.0403	.1456	.75	7	.4972	.1819	.95	7	.6386	.2006
.25	8	-.0089	-.0161	.75	8	.4621	-.0848	.95	8	.7325	-.1579
.25	9	-.0315	-.0933	.75	9	.0295	.1934	.95	9	.5280	-.3553
.25	10	.1313	-.1144	.75	10	.5656	.1112	.95	10	.6354	-.7540
.40	0	5.8900		.85	0	18.8383					
.40	1	-2.1594	3.1566	.85	1	1.2580	-2.0279				
.40	2	1.9841	-.1561	.85	2	5.4368	3.2310				
.40	3	-.5681	.7872	.85	3	.4740	.3303				
.40	4	-.2255	-.0809	.85	4	-.3039	-.5394				
.40	5	-.0558	-.0471	.85	5	-.8407	-.4136				
.40	6	.0791	-.0320	.85	6	.2935	1.1295				
.40	7	.0389	.0417	.85	7	.5486	.2879				
.40	8	-.0715	.0466	.85	8	.9387	-.6027				
.40	9	-.0231	-.1080	.85	9	.5826	-.3884				
.40	10	.0959	.0088	.85	10	.2903	-.2389				
.55	0	9.7770		.90	0	18.8995					
.55	1	-1.7673	2.6359	.90	1	2.4039	-3.4507				
.55	2	3.3321	1.2815	.90	2	4.4990	3.2885				
.55	3	.2178	.5155	.90	3	.4813	.6853				
.55	4	-.3748	.0910	.90	4	.3117	.3063				
.55	5	.1741	-.1092	.90	5	-.4551	.1736				
.55	6	.5937	.4302	.90	6	.6282	.7922				
.55	7	.1022	-.1865	.90	7	.8091	.1560				
.55	8	.2221	-.1647	.90	8	1.1051	-.3200				
.55	9	.1778	.0384	.90	9	.6563	-.6055				
.55	10	-.0273	.0849	.90	10	.4056	-.8793				

$$l = L_0 + \sum_{n=1}^{n} \left(L_n \cos n\psi_{nom} + M_n \sin n\psi_{nom} \right)$$

TABLE IV.- REDUCED FLIGHT TEST DATA FOR μ = 0.23 - Concluded

(e) Flapwise bending moment

ψ_{nom}, deg	Flapwise bending moment, in-lb, at -					
	r/R = 0.150	r/R = 0.275	r/R = 0.375	r/R = 0.450	r/R = 0.575	r/R = 0.650
0	340	-116	-99	-160	-1145	-3231
15	235	503	615	146	-969	-2554
30	5810	3185	1916	642	-1549	-3470
45	3610	3457	4502	3704	-124	-4226
60	4054	2516	2206	1472	105	-1589
75	2230	347	-45	-875	-2016	-2186
90	1011	-1757	-1962	-2068	-2130	-3241
105	1854	-850	-1690	-3203	-5703	-7191
120	2219	-635	-2667	-4586	-6381	-7211
135	-1041	-2236	-2323	-2945	-4365	-6962
150	919	-932	-2549	-3642	-4462	-6594
165	1387	8	-967	-2812	-4717	-7629
180	669	-380	-289	-789	-3389	-7450
195	1729	833	208	-1037	-4304	-7271
210	2344	1568	515	-1114	-3547	-5231
225	384	1576	1989	1109	-1356	-3649
240	1831	2054	2305	2121	721	-1480
255	1307	2830	3914	4048	2604	1037
270	1261	3308	4574	4887	5183	4540
285	1512	2945	4176	4649	4751	5485
300	1056	1733	2585	3304	4628	6072
315	-243	1378	2983	3933	4241	2828
330	1512	3647	4348	3246	-212	-4286
345	5035	3935	2748	375	-3670	-6385

(f) Chordwise bending moment

ψ_{nom}, deg	Chordwise bending moment, in-lb, at -		
	r/R = 0.150	r/R = 0.375	r/R = 0.575
0	-323	-9214	-6
15	19	-12405	-6086
30	-2228	-12145	-2278
45	2005	-2637	4666
60	6531	2458	12314
75	10943	7082	10874
90	4756	944	9146
105	2607	-5649	202
120	3144	-8107	-4326
135	19	-5731	2986
150	686	993	8458
165	1354	3679	11834
180	-1886	1351	11514
195	-5386	-5861	5722
210	-6510	-11119	-1766
225	-10970	-14017	-3014
240	-14389	-14408	-2358
255	-12436	-14196	-4886
270	-13363	-13171	-3590
285	-13396	-14050	-1718
300	-10173	-12259	-3270
315	-10921	-11445	4778
330	-5728	-1791	7306
345	-3140	-5356	6922

(g) Blade torsional moment and pitch horn load

ψ_{nom}, deg	Torsional moment, in-lb, at -		Pitch horn load, lb
	r/R = 0.150	r/R = 0.500	
0	2093	1324	275
15	2264	1808	264
30	999	532	205
45	1321	1129	165
60	1297	701	204
75	882	847	148
90	679	619	82
105	187	157	35
120	295	155	7
135	87	14	-38
150	-980	-648	-119
165	-908	-772	-84
180	-317	-169	-21
195	-291	-264	-52
210	-292	-552	-67
225	-1463	-1327	-194
240	-2022	-1935	-194
255	-845	-1122	-70
270	-3899	-3741	-294
285	-2518	-2186	-299
300	-34	-490	27
315	1289	35	270
330	-2282	-1835	-223
345	-2198	-1854	-199

TABLE V.- REDUCED FLIGHT DATA FOR μ = 0.11

(a) Differential pressures

ψ_{nom}, deg	Δp, lb/sq in., at -												ψ_{nom}, deg
	r/R = 0.95							r/R = 0.90					
	x/c=.017	x/c=.090	x/c=.168	x/c=.233	x/c=.335	x/c=.625	x/c=.915	x/c=.017	x/c=.090	x/c=.168	x/c=.233	x/c=.335	
0	5.459	3.837	2.924	1.930	.932	.456	.042	6.481	3.339	2.484	2.139	1.318	0
15	4.388	3.357	2.636	1.720	.718	.394	.026	5.513	2.859	2.161	1.876	1.122	15
30	3.066	3.120	2.515	1.591	.620	.371	.016	4.699	2.431	1.896	1.708	.987	30
45	3.278	2.850	2.363	1.427	.482	.327	.000	4.176	2.191	1.742	1.624	.880	45
60	2.367	2.209	2.011	1.079	.258	.229	-.024	3.102	1.640	1.352	1.255	.594	60
75	7.916	5.348	3.833	2.747	.909	.374	.016	1.571	.867	.970	1.025	.540	75
90	8.257	5.635	4.202	2.832	1.421	.637	.076	4.273	2.451	2.190	2.117	1.249	90
105	7.973	5.432	3.989	2.622	1.313	.570	.058	8.128	4.332	3.197	2.772	1.635	105
120	6.446	4.631	3.556	2.293	1.103	.512	.050	6.481	3.612	2.749	2.458	1.446	120
135	5.412	3.981	3.147	2.048	.978	.496	.056	6.753	3.580	2.690	2.352	1.380	135
150	5.127	3.728	2.874	1.957	.942	.484	.068	6.685	3.534	2.617	2.296	1.357	150
165	5.127	3.652	2.814	1.933	.942	.496	.075	6.811	3.534	2.639	2.313	1.364	165
180	5.317	3.728	2.828	1.965	.931	.508	.084	6.927	3.580	2.661	2.307	1.392	180
195	5.706	3.922	2.909	2.040	1.067	.536	.091	7.092	3.670	2.697	2.341	1.423	195
210	6.114	4.099	2.991	2.124	1.126	.558	.101	7.469	3.852	2.793	2.385	1.469	210
225	6.721	4.310	3.133	2.242	1.211	.594	.113	8.118	4.073	2.925	2.492	1.530	225
240	7.812	4.749	3.364	2.433	1.352	.629	.123	7.721	3.872	2.822	2.425	1.530	240
255	8.637	4.960	3.446	2.474	1.385	.618	.113	6.297	3.385	2.609	2.346	1.530	255
270	8.694	4.875	3.325	2.390	1.352	.606	.117	5.484	2.794	2.183	1.882	1.204	270
285	8.134	4.462	2.991	2.040	1.086	.524	.097	3.276	1.750	1.389	1.271	.821	285
300	4.757	3.205	2.419	1.631	.823	.418	.067	4.254	2.217	1.727	1.596	.994	300
315	5.706	3.753	2.821	1.711	.965	.484	.088	5.716	2.989	2.227	1.921	1.227	315
330	6.237	4.074	3.044	2.078	1.080	.524	.075	6.656	3.469	2.550	2.201	1.385	330
345	6.036	4.032	3.052	2.062	1.040	.500	.060	6.840	3.554	2.602	2.234	1.385	345

ψ_{nom}, deg	Δp, lb/sq in., at -												ψ_{nom}, deg
	r/R = 0.90		r/R = 0.85										
	x/c=.625	x/c=.915	x/c=.017	x/c=.040	x/c=.090	x/c=.130	x/c=.168	x/c=.233	x/c=.335	x/c=.500	x/c=.625	x/c=.769	
0	.492	-.006	6.617	4.883	3.552	2.594	2.220	1.870	1.209	.558	.541	.268	0
15	.406	-.034	5.883	4.323	3.200	2.234	1.982	1.672	1.074	.454	.476	.223	15
30	.362	-.060	5.193	3.784	2.867	2.133	1.701	1.460	.955	.365	.410	.190	30
45	.307	-.082	4.651	3.410	2.612	2.051	1.635	1.272	.846	.286	.345	.153	45
60	.199	-.125	3.741	2.729	2.152	1.605	1.377	.995	.686	.170	.266	.106	60
75	.255	-.101	3.066	2.190	1.741	1.293	1.085	1.077	.572	.109	.216	.080	75
90	.449	-.062	3.242	2.366	1.907	1.451	1.245	1.186	.707	.217	.315	.140	90
105	.617	-.022	4.313	3.311	2.710	2.195	1.830	1.511	1.066	.467	.491	.257	105
120	.561	-.005	7.130	5.279	3.885	2.766	2.376	1.932	1.269	.531	.501	.239	120
135	.522	-.020	5.237	3.949	3.102	2.248	1.943	1.672	1.160	.533	.535	.288	135
150	.527	-.002	6.367	4.674	3.445	2.469	2.130	1.774	1.186	.551	.535	.288	150
165	.544	.011	6.587	4.861	3.572	2.603	2.243	1.870	1.261	.598	.581	.317	165
180	.553	.018	6.734	4.938	3.621	2.646	2.251	1.887	1.266	.607	.590	.317	180
195	.570	.034	6.558	4.894	3.503	2.570	2.189	1.836	1.235	.610	.600	.330	195
210	.591	.045	5.839	4.388	3.249	2.397	2.064	1.764	1.212	.620	.606	.338	210
225	.603	.051	5.531	4.125	3.063	2.267	1.970	1.702	1.183	.622	.600	.348	225
240	.629	.060	6.382	4.641	3.445	2.613	2.196	1.880	1.280	.666	.626	.354	240
255	.700	.105	5.282	3.806	2.867	2.090	1.775	1.497	1.026	.504	.501	.263	255
270	.522	.045	3.741	2.740	2.064	1.538	1.233	1.114	.789	.360	.410	.226	270
285	.380	.011	3.711	2.696	1.986	1.552	1.155	1.050	.703	.299	.355	.184	285
300	.419	.016	4.988	3.663	2.573	1.840	1.584	1.391	.895	.420	.440	.239	300
315	.509	.038	6.133	4.575	3.200	2.363	1.994	1.726	1.104	.546	.525	.283	315
330	.556	.038	7.028	5.213	3.699	2.718	2.302	1.966	1.261	.646	.581	.309	330
345	.535	.016	7.028	5.257	3.699	2.733	2.310	1.969	1.269	.634	.575	.293	345

TABLE V.- REDUCED FLIGHT DATA FOR μ = 0.11 - Continued

(a) Differential pressures - Concluded

ψ_{nom}, deg	Δp, lb/sq in., at -												ψ_{nom}, deg
	r/R = 0.85	r/R = 0.75							r/R = 0.55				
	x/c=.915	x/c=.017	x/c=.090	x/c=.168	x/c=.233	x/c=.335	x/c=.625	x/c=.915	x/c=.017	x/c=.090	x/c=.168	x/c=.233	
0	.062	5.556	2.948	2.226	1.735	1.162	.495	.055	3.377	1.698	1.116	1.015	0
15	.042	5.210	2.718	2.100	1.637	1.061	.446	.050	3.295	1.641	1.097	.989	15
30	.023	4.820	2.538	1.999	1.567	.991	.415	.044	3.239	1.607	1.065	.975	30
45	.008	4.419	2.338	1.903	1.483	.905	.376	.050	2.999	1.465	.987	.914	45
60	-.012	3.924	1.992	1.621	1.315	.773	.316	.031	2.709	1.364	.865	.826	60
75	-.033	3.463	1.792	1.408	1.205	.677	.280	.024	2.432	1.260	.764	.752	75
90	-.014	3.446	1.882	1.442	1.245	.688	.293	.029	2.520	1.288	.781	.757	90
105	.035	3.315	1.902	1.442	1.238	.747	.306	.039	2.539	1.288	.798	.760	105
120	.023	4.117	2.408	1.922	1.501	.937	.391	.053	2.388	1.219	.747	.733	120
135	.060	3.683	2.032	1.654	1.431	.944	.436	.082	2.300	1.159	.732	.717	135
150	.058	4.419	2.613	2.097	1.617	1.053	.425	.055	2.092	1.052	.650	.666	150
165	.070	4.996	2.753	2.113	1.637	1.057	.430	.061	1.821	.904	.587	.598	165
180	.074	5.248	2.678	2.054	1.588	1.057	.428	.055	1.638	.806	.559	.560	180
195	.081	5.116	2.623	1.999	1.540	1.010	.410	.053	1.613	.781	.520	.547	195
210	.089	5.204	2.678	1.987	1.523	.991	.399	.053	1.676	.822	.532	.561	210
225	.105	4.611	2.112	1.731	1.431	.948	.407	.048	1.859	.876	.619	.621	225
240	.105	3.435	1.627	1.298	1.033	.700	.340	.055	1.928	.923	.637	.642	240
255	.056	3.304	1.757	1.436	1.114	.735	.327	.037	1.966	.948	.648	.643	255
270	.045	3.282	1.707	1.392	1.081	.705	.316	.034	1.934	.923	.637	.635	270
285	.035	3.260	1.737	1.387	1.087	.668	.308	.037	1.997	.948	.648	.643	285
300	.056	3.644	2.032	1.581	1.232	.796	.360	.046	2.211	1.074	.720	.698	300
315	.081	4.287	2.473	1.876	1.468	.976	.436	.061	2.571	1.276	.844	.791	315
330	.093	4.974	2.863	2.143	1.680	1.142	.500	.063	3.037	1.528	1.008	.925	330
345	.076	5.457	2.979	2.242	1.750	1.185	.508	.055	3.245	1.641	1.080	.988	345

ψ_{nom}, deg	Δp, lb/sq in., at -													ψ_{nom}, deg
	r/R = 0.55			r/R = 0.40					r/R = 0.25					
	x/c=.335	x/c=.625	x/c=.915	x/c=.042	x/c=.158	x/c=.300	x/c=.600	x/c=.910	x/c=.042	x/c=.158	x/c=.300	x/c=.600	x/c=.910	
0	.813	.405	.105	1.577	.847	.503	.304	.090	.664	.314	.192	.141	.025	0
15	.794	.399	.108	1.613	.843	.499	.303	.093	.832	.417	.252	.161	.029	15
30	.786	.392	.107	1.674	.854	.507	.303	.095	.859	.407	.239	.154	.025	30
45	.741	.377	.102	1.635	.817	.488	.293	.099	.805	.377	.220	.141	.026	45
60	.674	.342	.101	1.488	.747	.447	.271	.096	.771	.358	.200	.132	.026	60
75	.633	.322	.101	1.361	.671	.409	.266	.095	.712	.321	.186	.123	.024	75
90	.633	.316	.101	1.278	.656	.392	.269	.095	.656	.296	.171	.118	.023	90
105	.629	.306	.099	1.325	.660	.397	.267	.093	.666	.306	.175	.122	.024	105
120	.617	.293	.098	1.330	.663	.402	.261	.091	.728	.331	.192	.127	.031	120
135	.593	.287	.093	1.283	.656	.394	.260	.090	.727	.336	.186	.123	.029	135
150	.566	.274	.092	1.189	.611	.359	.242	.085	.680	.309	.170	.114	.026	150
165	.515	.262	.087	1.048	.547	.318	.224	.076	.599	.270	.151	.109	.025	165
180	.491	.245	.083	.909	.502	.283	.211	.070	.535	.240	.136	.103	.025	180
195	.467	.245	.075	.862	.484	.275	.204	.067	.460	.206	.115	.097	.016	195
210	.455	.236	.071	.843	.480	.270	.202	.064	.391	.168	.093	.087	.013	210
225	.494	.245	.068	.807	.463	.264	.195	.061	.329	.130	.070	.078	.006	225
240	.513	.258	.065	.812	.463	.260	.190	.057	.296	.115	.059	.075	.008	240
255	.521	.255	.063	.840	.474	.259	.190	.051	.300	.116	.062	.074	.005	255
270	.509	.255	.057	.856	.487	.262	.189	.056	.310	.117	.063	.077	.003	270
285	.513	.753	.058	.892	.495	.268	.192	.058	.321	.125	.065	.079	.002	285
300	.549	.271	.063	.959	.526	.291	.203	.064	.364	.150	.079	.088	.007	300
315	.621	.310	.075	1.086	.602	.352	.234	.076	.474	.210	.115	.103	.012	315
330	.719	.363	.090	1.291	.715	.429	.275	.089	.556	.265	.157	.121	.016	330
345	.779	.390	.098	1.488	.810	.483	.299	.091	.580	.231	.171	.127	.023	345

TABLE V.- REDUCED FLIGHT TEST DATA FOR μ = 0.11 - Continued

(b) Section aerodynamic loading

ψ_{nom}, deg	Section aerodynamic loading, l, lb/in., at -						
	r/R = 0.25	r/R = 0.40	r/R = 0.55	r/R = 0.75	r/R = 0.85	r/R = 0.90	r/R = 0.95
0	3.215	7.904	12.297	19.074	21.177	21.213	20.259
15	4.009	7.947	12.029	17.646	18.827	18.011	17.157
30	3.934	8.102	11.821	16.507	16.519	15.581	15.711
45	3.655	7.864	11.056	15.273	14.783	13.873	13.836
60	3.443	7.220	10.060	13.108	11.915	9.854	10.211
75	3.175	6.716	9.318	11.592	9.808	7.234	24.950
90	2.955	6.511	9.377	11.901	11.518	17.353	29.816
105	3.029	6.594	9.337	12.135	16.745	26.862	28.104
120	3.288	6.583	8.935	15.389	22.102	22.984	24.045
135	3.242	6.456	8.628	14.528	18.853	22.492	21.205
150	2.999	5.977	8.020	16.790	20.537	22.253	20.079
165	2.701	5.354	7.235	17.492	21.636	22.547	19.968
180	2.457	4.828	6.718	17.427	21.911	22.886	20.478
195	2.134	4.640	6.495	16.884	21.478	23.452	21.653
210	1.809	4.562	6.518	16.868	20.379	24.439	22.712
225	1.484	4.401	7.055	15.148	19.658	25.753	24.237
240	1.355	4.351	7.333	11.590	21.691	25.182	26.770
255	1.357	4.390	7.414	11.901	17.561	23.698	27.807
270	1.389	4.461	7.275	11.572	13.021	19.120	27.346
285	1.435	4.579	10.111	11.425	12.116	12.416	24.261
300	1.668	4.910	8.079	13.216	15.840	15.259	17.491
315	2.184	5.689	9.344	15.920	19.565	19.620	20.572
330	2.681	6.777	11.011	18.375	22.352	22.376	22.374
345	2.858	7.599	11.835	19.226	22.301	22.527	21.854

(c) Harmonic analysis of blade root motion

Pitch motion			Flap motion			Lag motion		
n	$A_{n,s}$, deg	$B_{n,s}$, deg	n	$a_{n,s}$, deg	$b_{n,s}$, deg	n	E_n, deg	F_n, deg
0	10.6690	--	0	3.1792	--	0	4.9141	--
1	1.4891	-1.5754	1	.7999	-.6379	1	-.1382	-.0016
2	.6311	.4177	2	-.0284	.2349	2	.0110	.0440
3	.5039	-.4086	3	.1620	-.1316	3	.0298	.0204
4	-.3087	-.6447	4	.1114	.0709	4	.0079	0
5	-.6855	.2043	5	-.0324	-.0182	5	.0094	.0063
6	.0182	.7173	6	.0365	.0041	6	.0031	.0047
7	.6628	.1907	7	.0304	.0061	7	.0126	.0126
8	.3496	-.5857	8	.0122	.0101	8	.0047	.0031
9	-.4676	-.4767	9	.0223	0	9	.0094	.0031
10	-.5947	.3632	10	.0365	0	10	.0094	.0047
$\theta_s = A_o + \sum_{n=1}^{n}\left(A_{n,s} \cos n\,\psi_{nom} + B_{n,s} \sin n\psi_{nom}\right)$			$\beta_s = a_o + \sum_{n=1}^{n}\left(a_{n,s} \cos n\,\psi_{nom} + b_{n,s} \sin n\,\psi_{nom}\right)$			$\zeta = E_o + \sum_{n=1}^{n}\left(E_n \cos n\psi_{nom} + F_n \sin n\psi_{nom}\right)$		

TABLE V.- REDUCED FLIGHT TEST DATA FOR $\mu = 0.11$ - Continued

(d) Harmonic analysis of section aerodynamic loading

r/R	n	L_n, lb/in.	M_n, lb/in.	r/R	n	L_n, lb/in.	M_n, lb/in.	r/R	n	L_n, lb/in.	M_n, lb/in.
.25	0	2.6023		.75	0	15.0411		.95	0	21.7873	
.25	1	.4470	1.0018	.75	1	.4666	.1493	.95	1	-2.3256	-1.5373
.25	2	.3754	-.0036	.75	2	3.4666	-.5073	.95	2	-3.0378	-1.0373
.25	3	.0651	.1635	.75	3	.3095	-.3451	.95	3	2.7990	-1.9902
.25	4	-.0657	.0532	.75	4	-.2221	-.0003	.95	4	2.6024	-.2079
.25	5	-.0514	-.0137	.75	5	-.0959	-.3149	.95	5	-.5870	.6236
.25	6	-.0284	.0782	.75	6	-.1840	-.1856	.95	6	-1.5653	.0903
.25	7	-.0440	.0369	.75	7	.1392	.3251	.95	7	-.6962	-.4573
.25	8	-.0297	.0213	.75	8	.0642	-.3060	.95	8	.4312	-.2837
.25	9	-.0167	.0173	.75	9	.0741	.0340	.95	9	1.0166	-.0292
.25	10	-.0150	.0101	.75	10	-.0255	.3149	.95	10	.4969	.2017
.25	11	-.0209	.0020	.75	11	-.0700	-.2760	.95	11	-.3161	.2696
.25	12	-.0029		.75	12	.1102		.95	12	-.3463	
.40	0	6.0172		.85	0	18.0122					
.40	1	1.2318	1.2343	.85	1	-1.5492	-1.2674				
.40	2	.4800	-.0089	.85	2	3.9105	-1.2901				
.40	3	.3066	.1135	.85	3	2.1332	-.6881				
.40	4	-.0864	-.0337	.85	4	-.8886	-.2740				
.40	5	-.0211	-.1129	.85	5	-1.3760	-.1131				
.40	6	-.0495	-.0460	.85	6	.8591	-.0955				
.40	7	.0070	-.0273	.85	7	.2123	.1030				
.40	8	-.0030	-.0095	.85	8	-.4514	-.0350				
.40	9	.0067	-.0014	.85	9	.4174	.0071				
.40	10	.0094	-.0071	.85	10	-.1324	.2003				
.40	11	.0069	.0087	.85	11	-.2047	-.0368				
.40	12	-.0017		.85	12	.2346					
.55	0	9.0542		.90	0	19.8743					
.55	1	2.2928	.8347	.90	1	-3.7057	-1.8802				
.55	2	.4224	-.1469	.90	2	2.2875	-1.2694				
.55	3	.4703	.1995	.90	3	4.1505	-1.3324				
.55	4	.0485	.0793	.90	4	-.1463	.2406				
.55	5	.1004	-.0810	.90	5	-2.2061	.0781				
.55	6	-.0500	-.2834	.90	6	-.3120	-.7892				
.55	7	-.2118	-.1069	.90	7	1.2669	.0237				
.55	8	-.0854	.2340	.90	8	.4143	.4431				
.55	9	.1476	.1645	.90	9	-.5871	-.1301				
.55	10	.2183	-.1017	.90	10	-.0690	-.1413				
.55	11	-.0099	-.2254	.90	11	.2451	.2599				
.55	12	-.1005		.90	12	.0006					

$$l = L_o + \sum_{n=1}^{n} \left(L_n \cos n\psi_{nom} + M_n \sin n\psi_{nom}\right)$$

TABLE V.- REDUCED FLIGHT TEST DATA FOR μ = 0.11 - Concluded

(e) Flapwise bending moment

ψ_{nom}, deg	Flapwise bending moment, in-lb, at -					
	r/R = 0.150	r/R = 0.275	r/R = 0.375	r/R = 0.450	r/R = 0.575	r/R = 0.650
0	-840	-1262	-1835	-2900	-4590	-6952
15	699	-173	-922	-2194	-3992	-5997
30	1075	644	271	-582	-2504	-4415
45	859	512	389	115	-454	-1808
60	551	578	551	-19	-903	-1718
75	1189	503	-18	-772	-2425	-3549
90	574	17	-994	-2337	-3235	-3490
105	-327	-1460	-2133	-2499	-1501	-1201
120	-680	-1172	-994	-906	-49	-246
135	1611	1081	1148	821	479	-733
150	2785	2434	2911	2471	1121	-1022
165	2113	1799	2378	2309	1834	212
180	859	685	1112	1050	945	282
195	768	140	118	-76	-137	-1002
210	847	437	289	-219	-1316	-2863
225	1486	899	434	-276	-1519	-2883
240	1235	784	533	10	-454	-1022
255	574	578	741	744	1262	1655
270	893	1213	1573	1679	2424	3058
285	1258	2228	2857	2805	2371	2102
300	1566	2351	2875	2433	1156	262
315	1269	1370	1410	983	-894	-2783
330	277	223	-362	-1641	-3516	-5062
345	175	-949	-2097	-3281	-4696	-6285

(f) Chordwise bending moment

ψ_{nom}, deg	Chordwise bending moment, in-lb, at -		
	r/R = 0.150	r/R = 0.375	r/R = 0.575
0	-5539	-7261	2781
15	-6060	-8677	621
30	-6516	-8970	989
45	-5621	-7586	3037
60	-3163	-4868	4253
75	-2169	-3354	5885
90	-867	-3126	4637
105	1559	-5910	1405
120	761	-7912	-1027
135	-1046	-9491	-195
150	-509	-6838	1357
165	-37	-4103	4733
180	-297	-2556	7069
195	93	-3354	5005
210	-1388	-6789	2285
225	-3423	-9117	-707
240	-4611	-10208	-1891
255	-6028	-10452	-1203
270	-8584	-9833	29
285	-11319	-10501	2109
300	-10537	-9198	2669
315	-8502	-7245	3757
330	-5686	-5649	4413
345	-4481	-4786	4029

(g) Blade torsional moment and pitch horn load

ψ_{nom}, deg	Torsional moment, in-lb, at -		Pitch horn load, lb
	r/R = 0.150	r/R = 0.500	
0	432	567	118
15	275	359	113
30	395	398	121
45	380	344	125
60	371	380	118
75	483	559	124
90	692	782	147
105	761	722	124
120	348	320	80
135	314	63	57
150	296	101	52
165	218	63	38
180	-41	-8	10
195	-147	-65	-5
210	-68	-112	-3
225	-57	-58	7
240	-40	-46	8
255	-253	-238	3
270	-368	-274	1
285	-442	-320	3
300	-362	-214	12
315	-271	-72	33
330	-28	175	76
345	274	443	111

Figure 1.- Test helicopter. L-61-4196

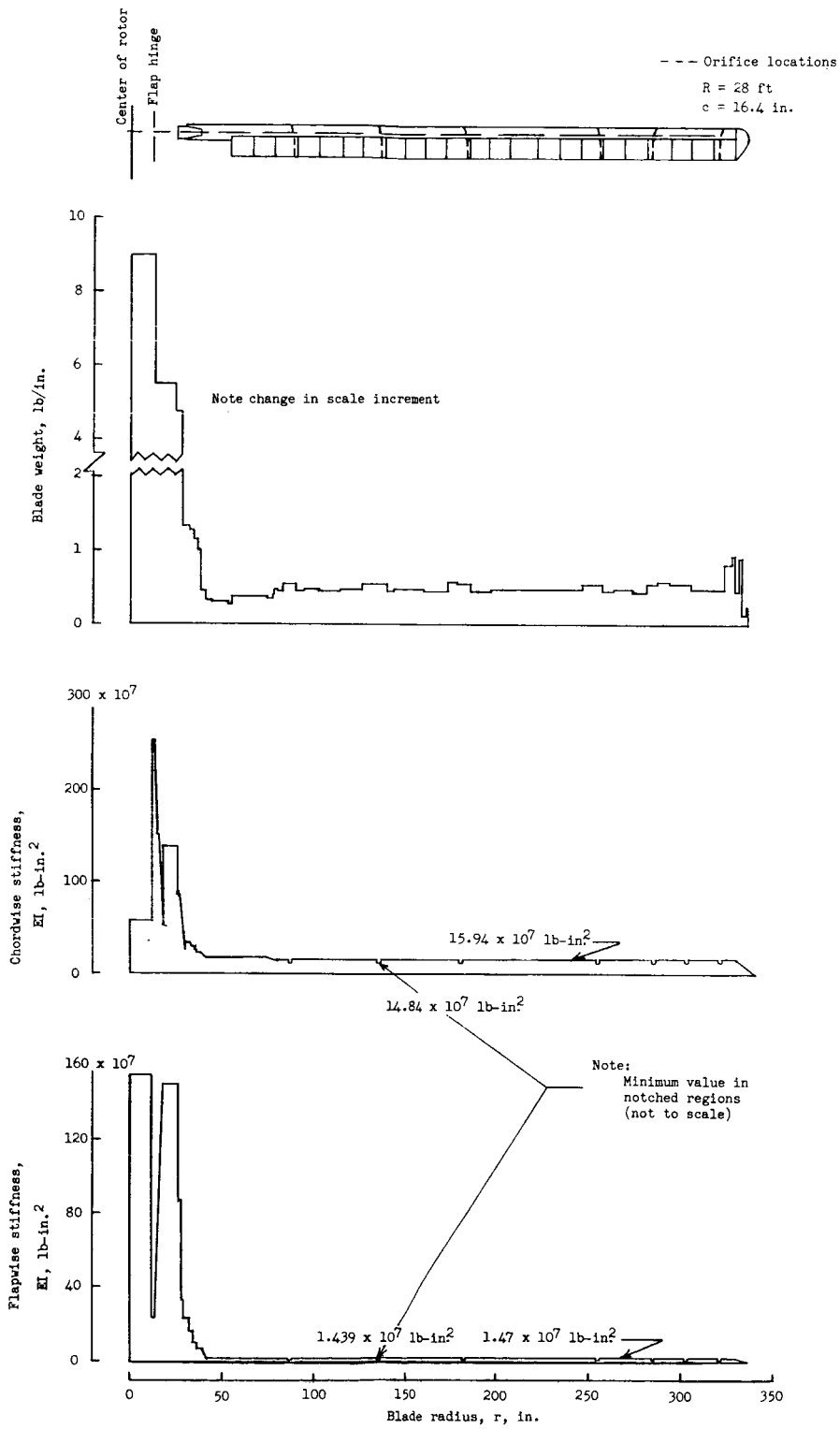

Figure 2.- Weight and stiffness distributions.

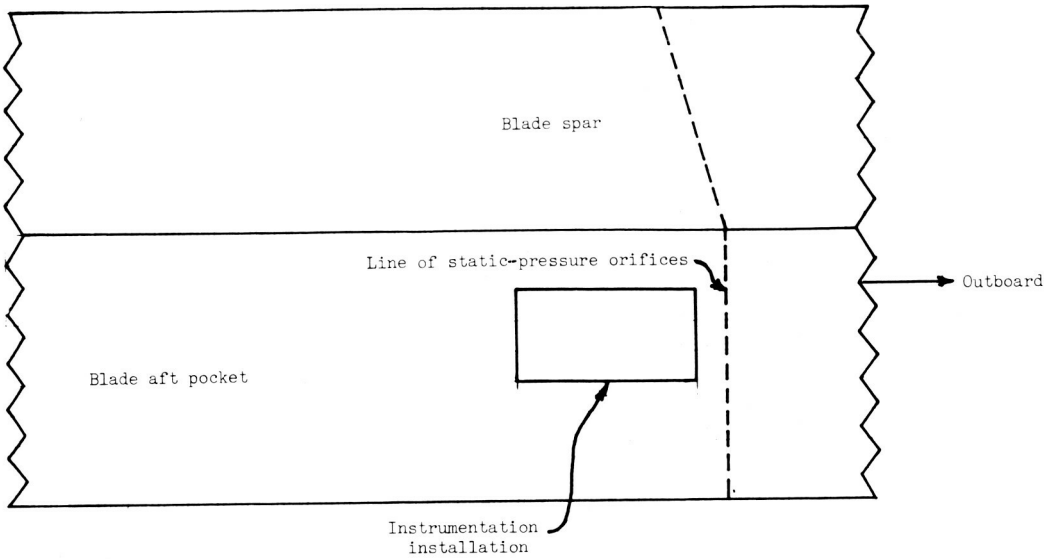

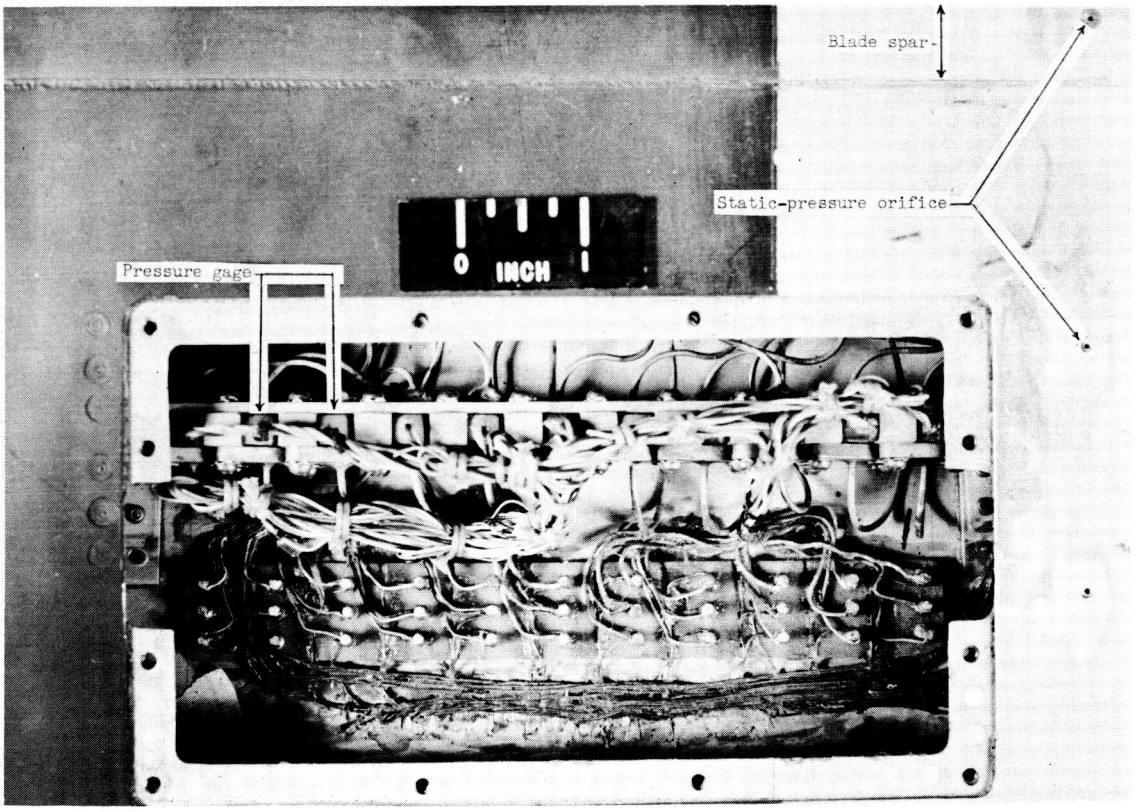

L-61-327

Figure 3.- Blade section and photograph of top surface of blade showing pressure-gage and wiring installation.

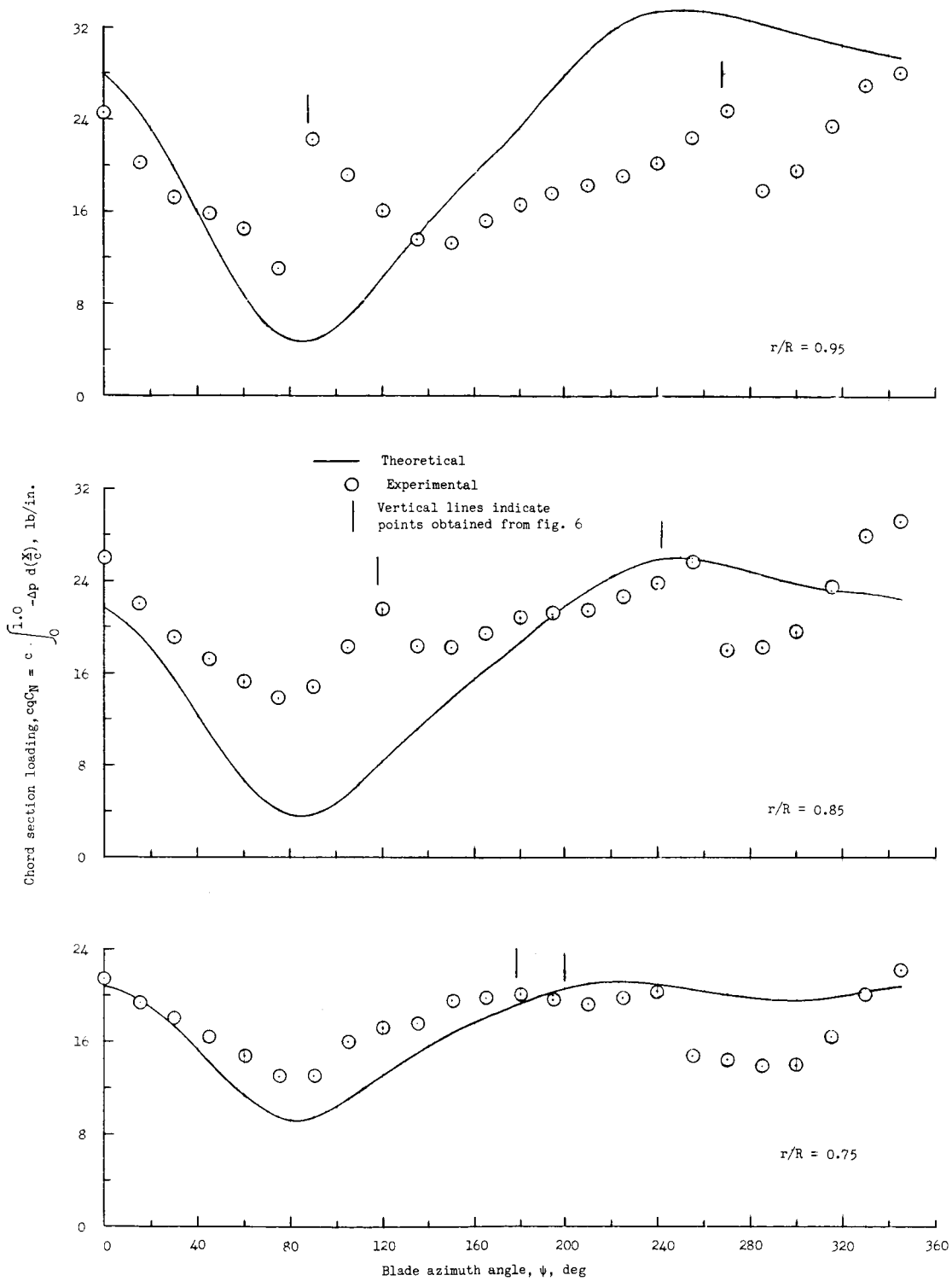

Figure 4.- Blade-section loading as a function of azimuth angle. $\mu = 0.18$.

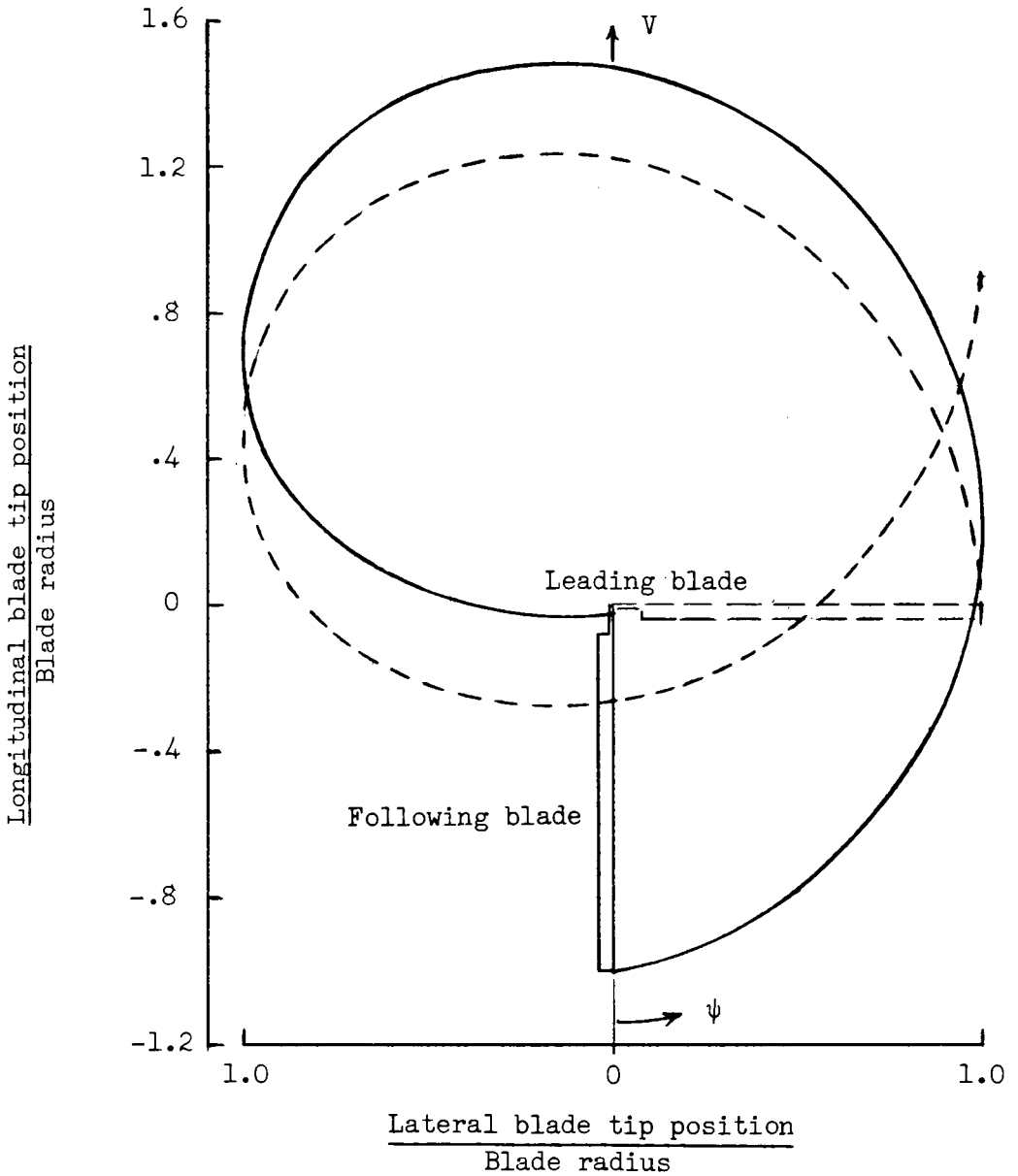

Figure 5.- Blade tip path of two succeeding blades as viewed from above. $\mu = 0.18$.

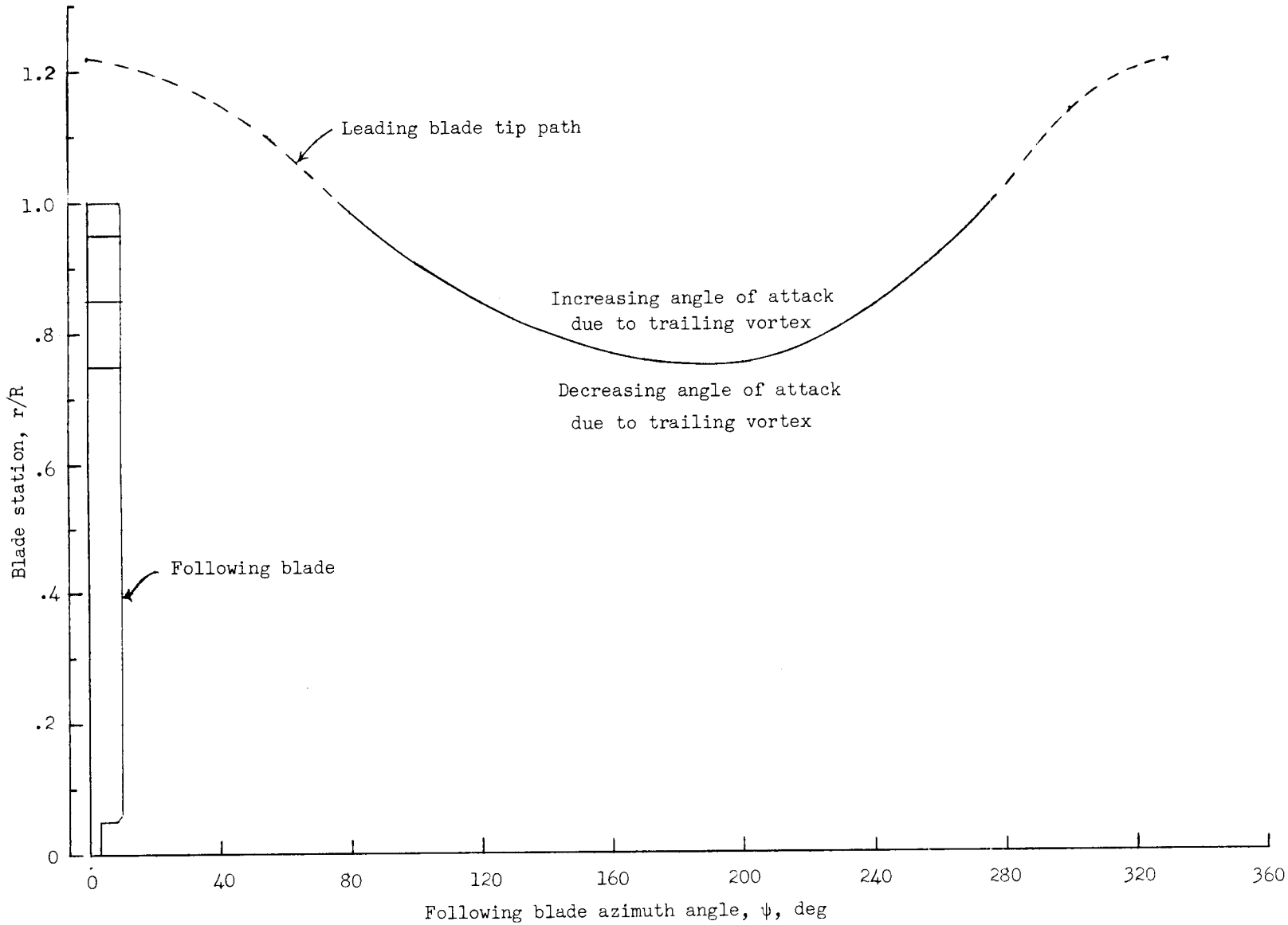

Figure 6.- Calculated spanwise blade station of the following blade that would strike the tip path of the leading blade. $\mu = 0.18$.

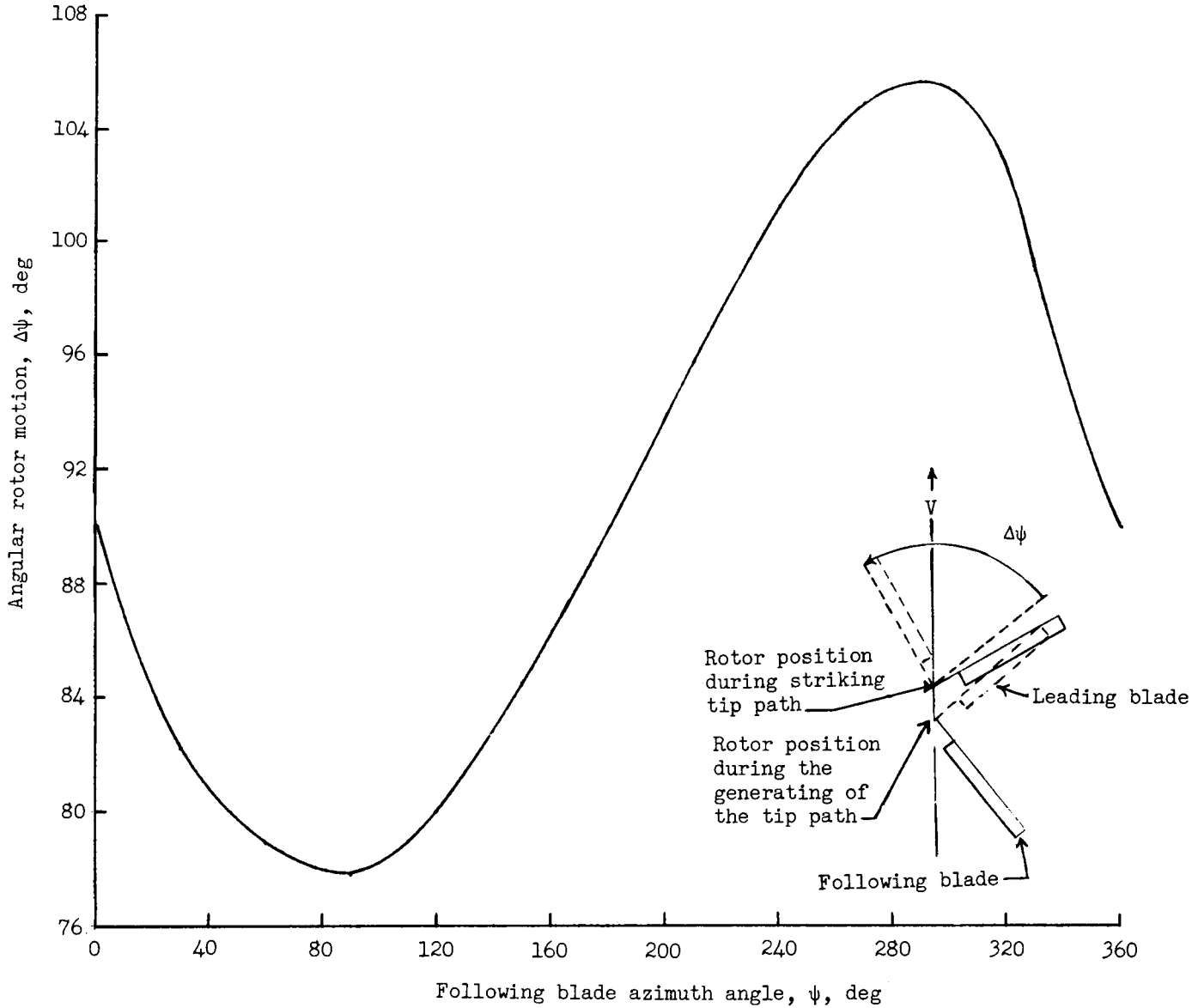

Figure 7.- Angular rotation between the generating of the tip path of the leading blade and the striking of the tip path by the following blade. $\mu = 0.18$.

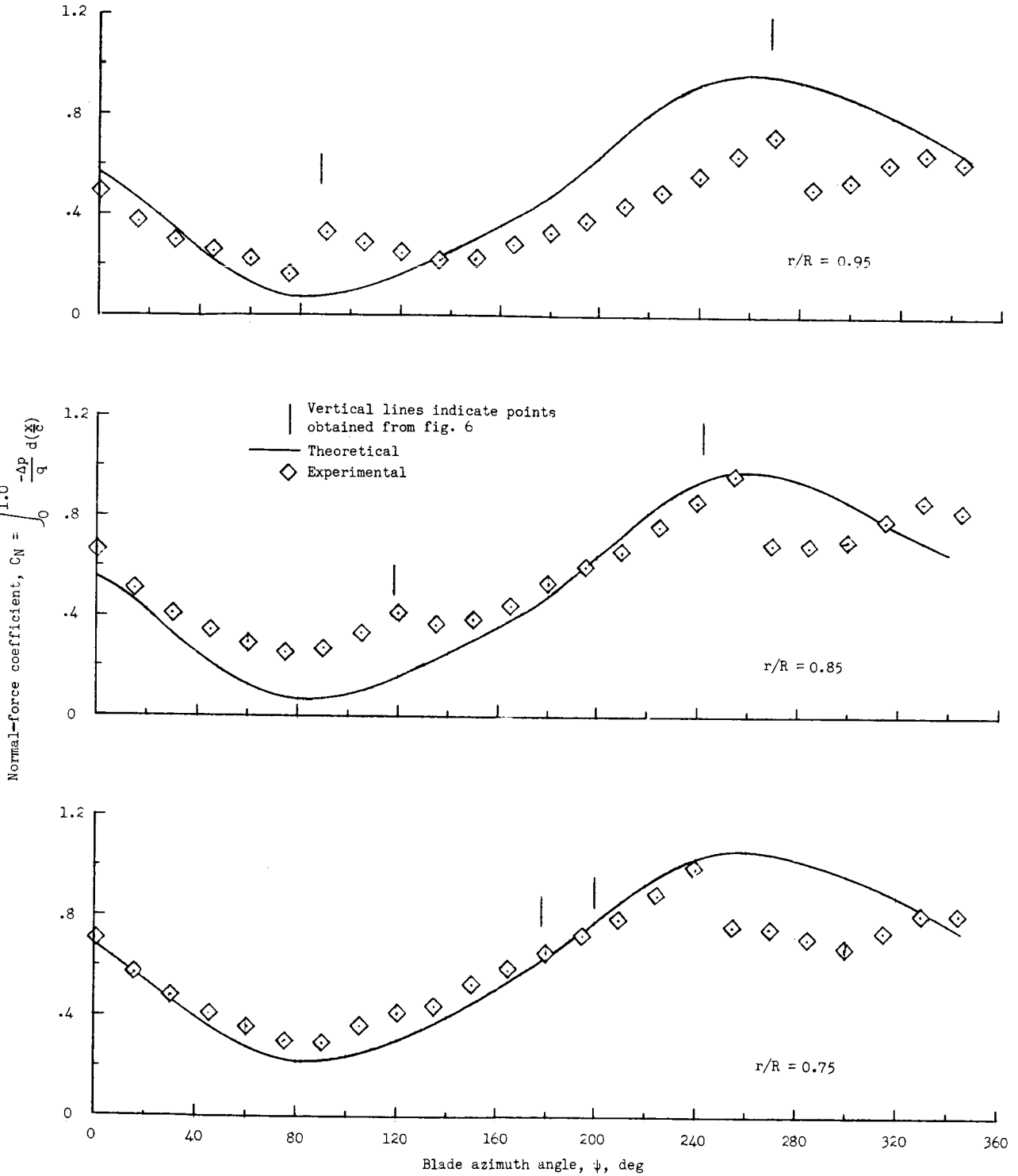

Figure 8.- Blade normal-force coefficient as a function of azimuth angle. $\mu = 0.18$.

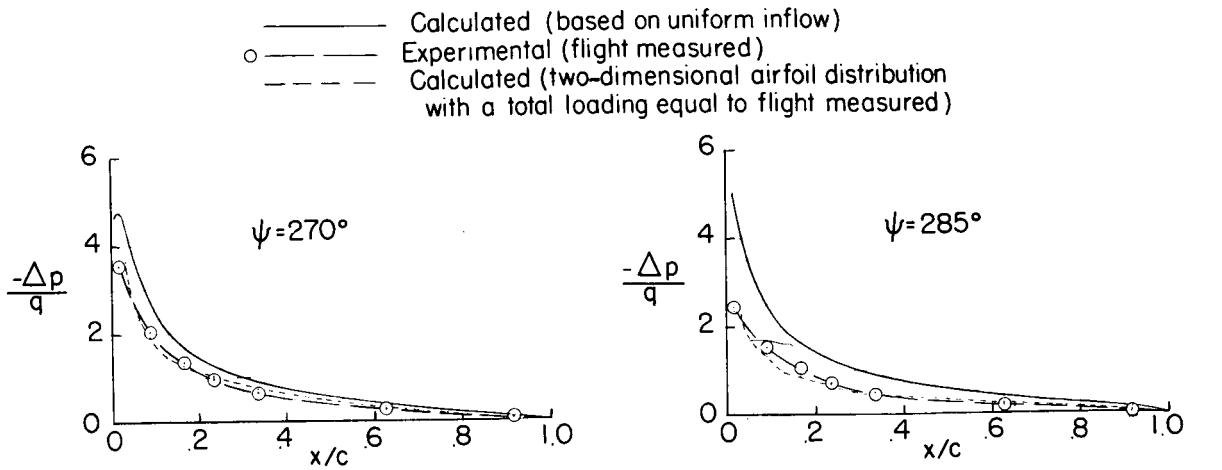

(a) r/R = 0.95.

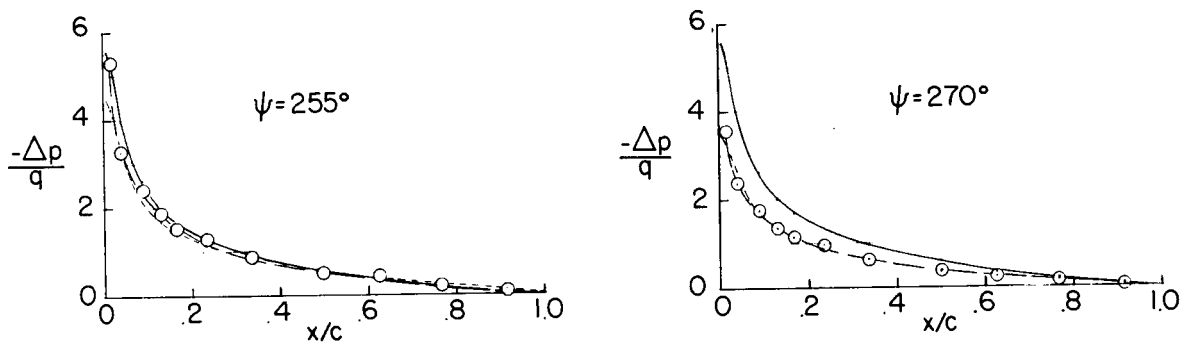

(b) r/R = 0.85.

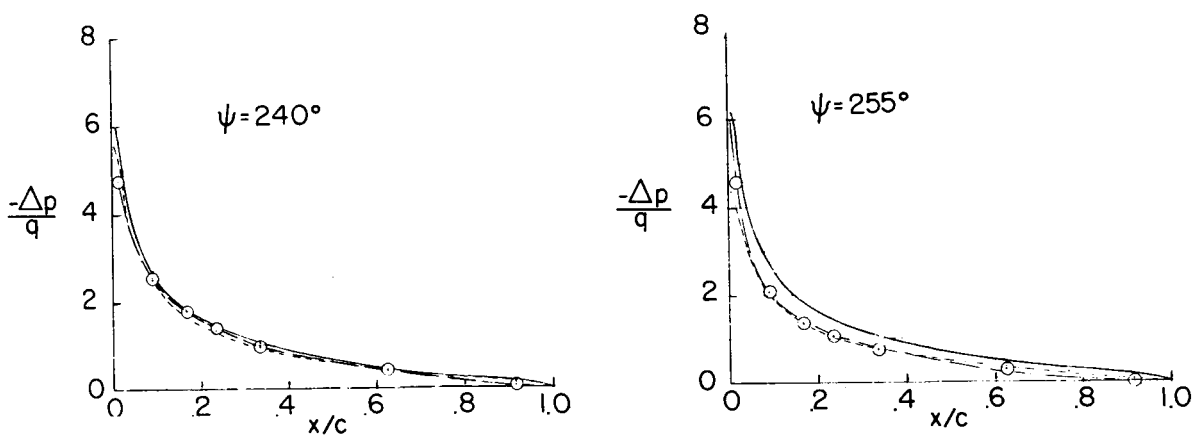

(c) r/R = 0.75.

Figure 9.- Chordwise pressure distribution. μ = 0.18.

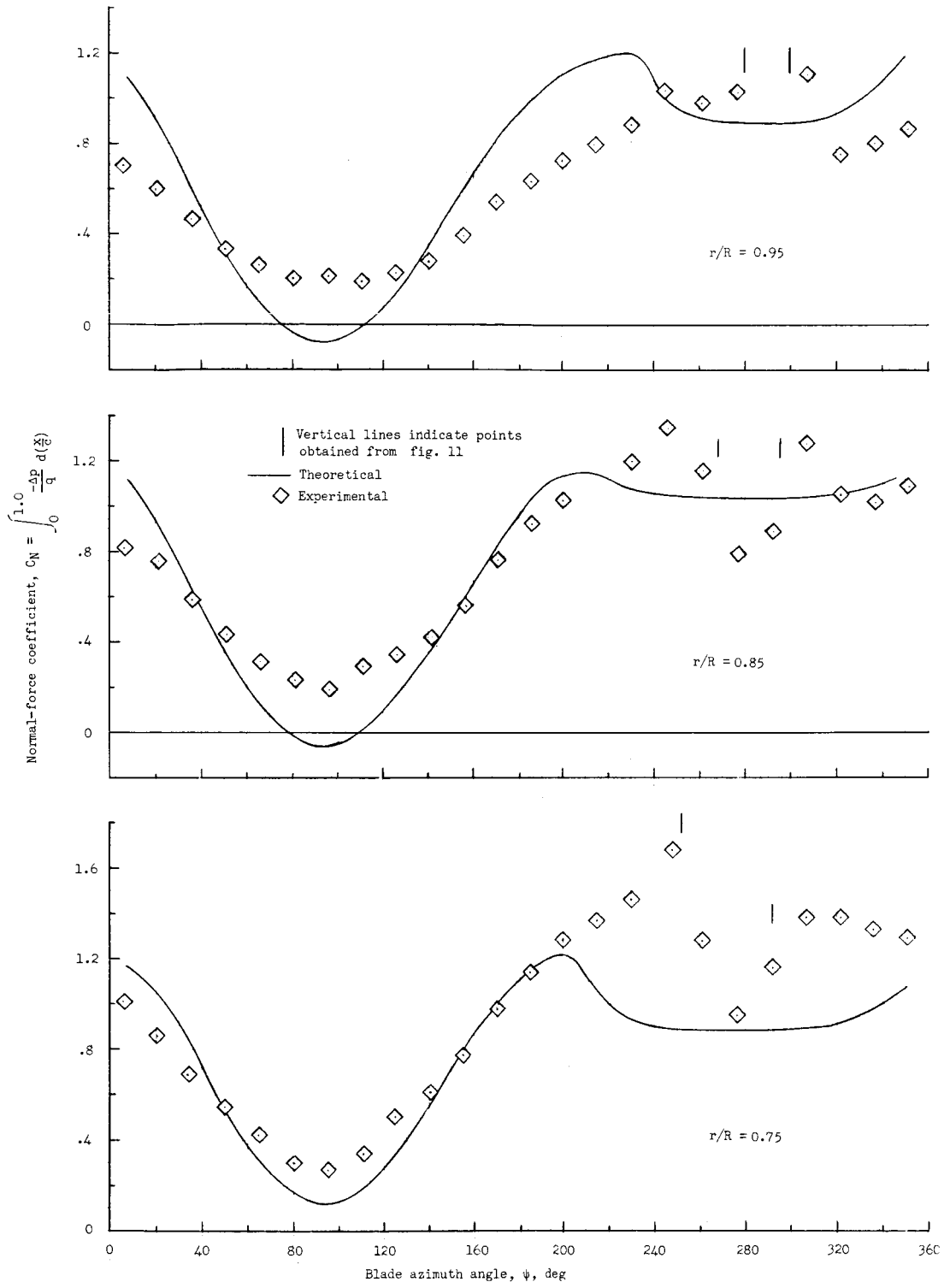

Figure 10.- Blade normal-force coefficient as a function of azimuth angle. $\mu = 0.23$.

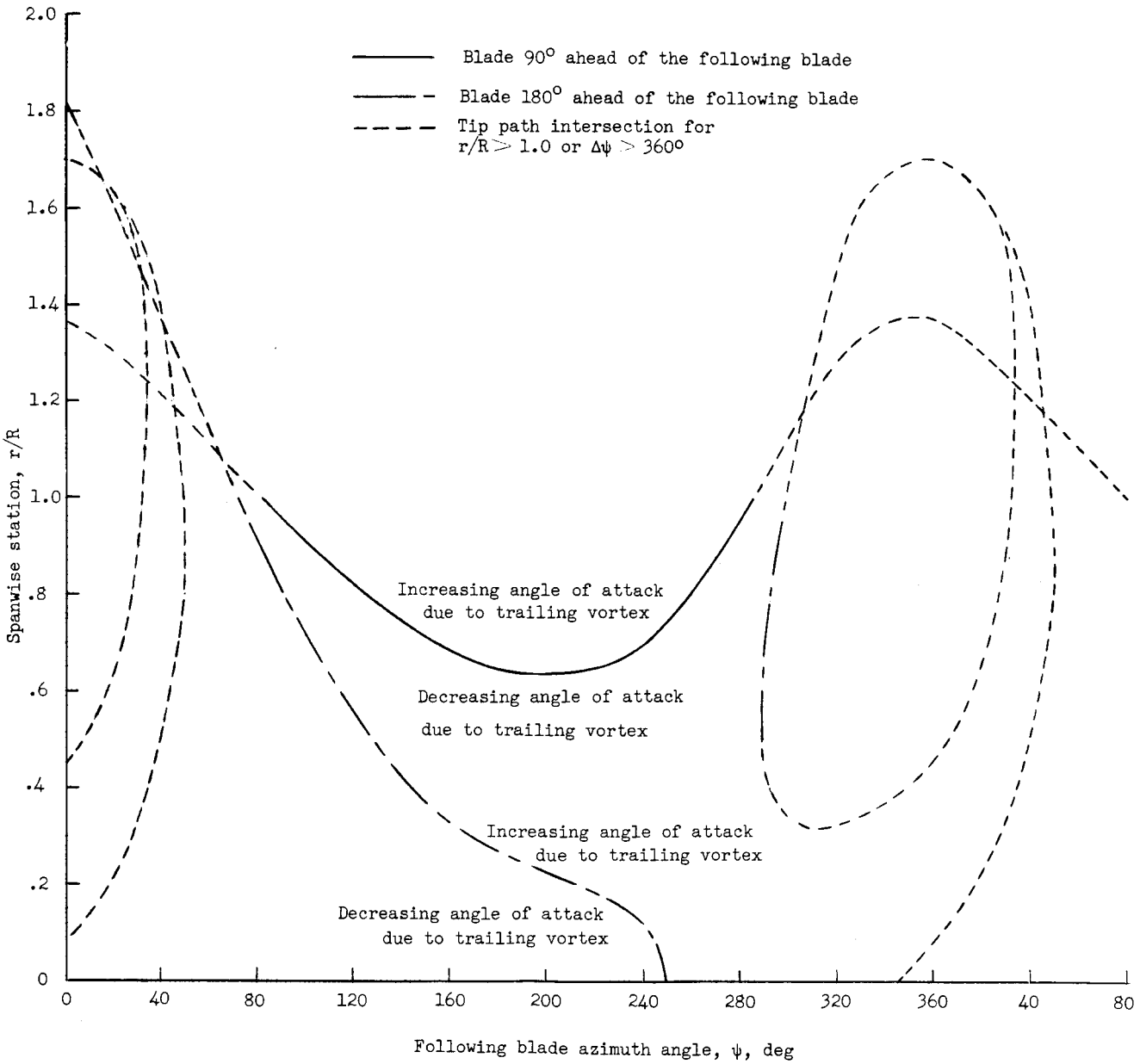

Figure 11.- Calculated spanwise blade station of the following blade that would strike the tip path of the two leading blades. $\mu = 0.23$.

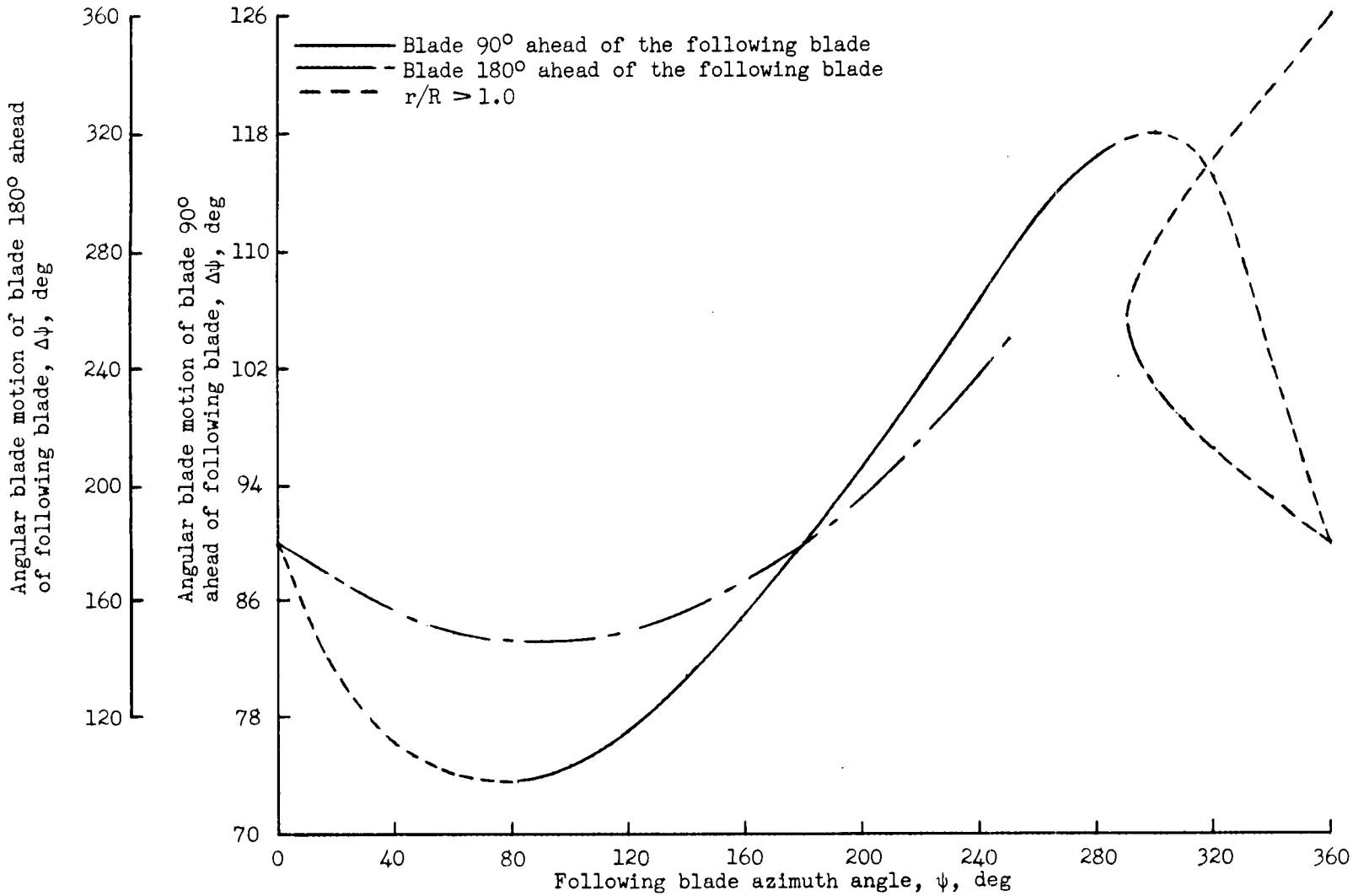

Figure 12.- Angular rotation between the shedding of the tip vortices of two leading blades and the striking of the tip path by the following blade. $\mu = 0.23$.

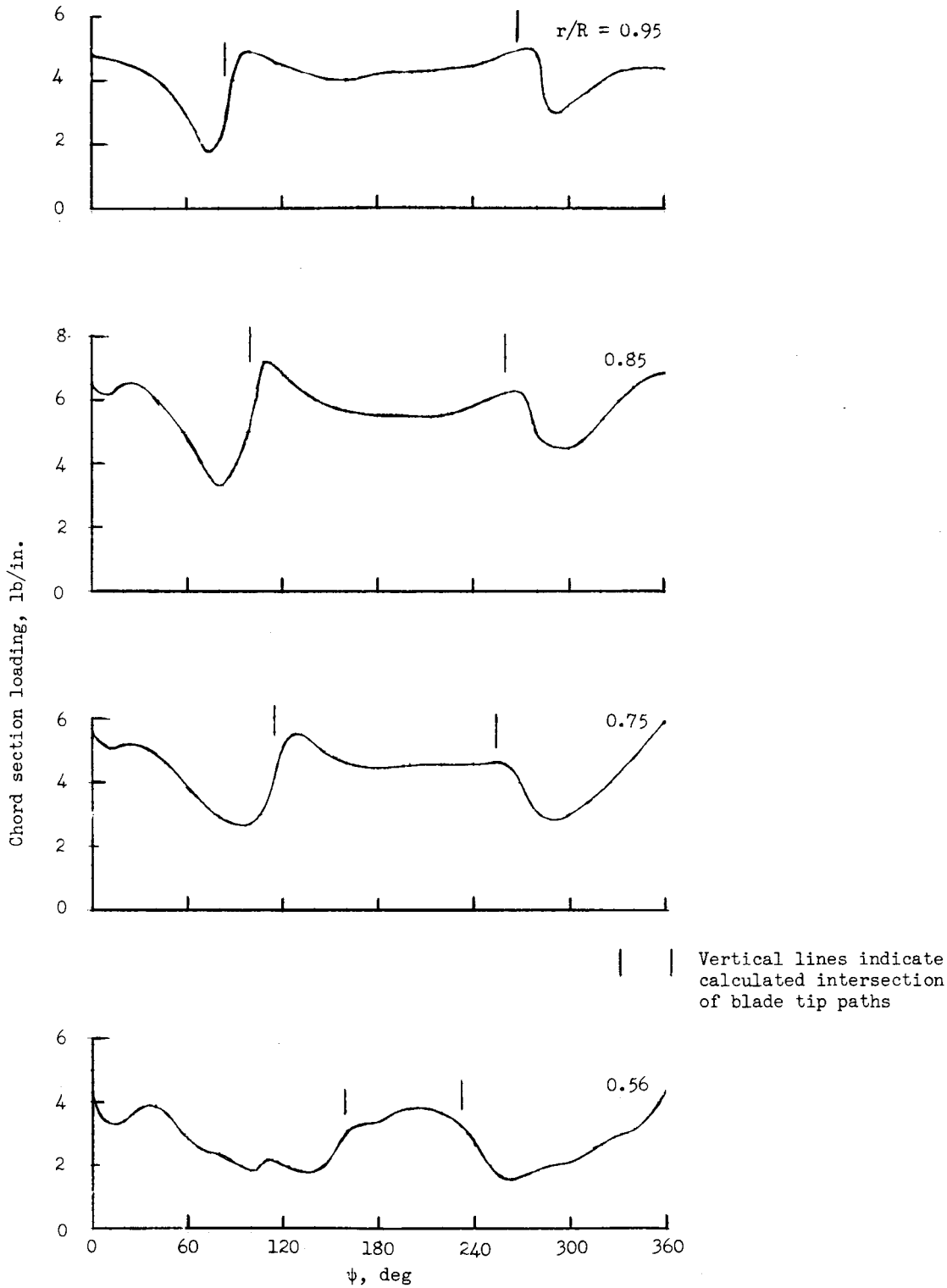

Figure 13.- Blade-section loading as a function of azimuth angle for a two-blade rotor (ref. 7).

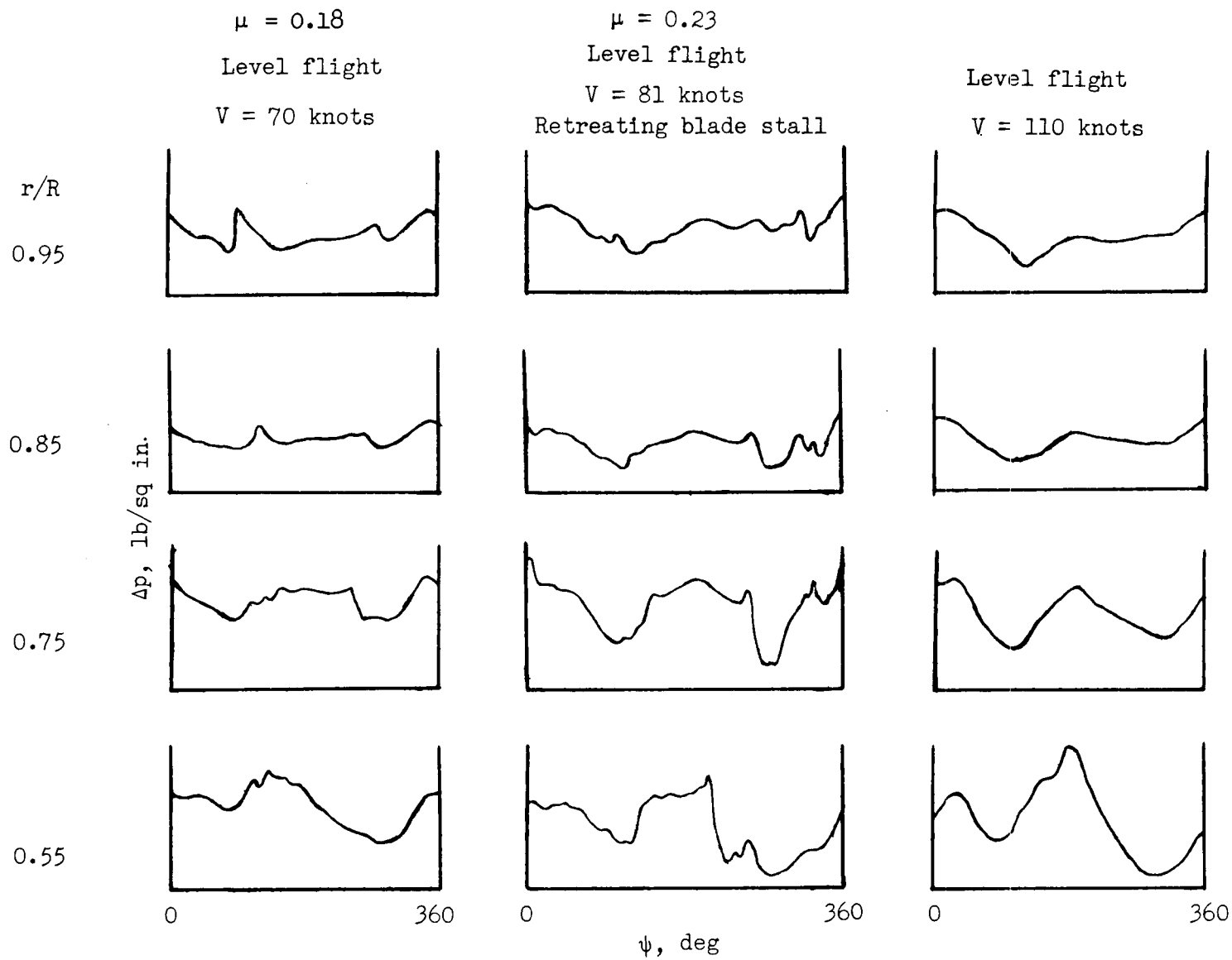

Figure 14.- Sample records of rotor-blade response as a function of blade azimuth angle. All pressure readings at x/c = 0.090.

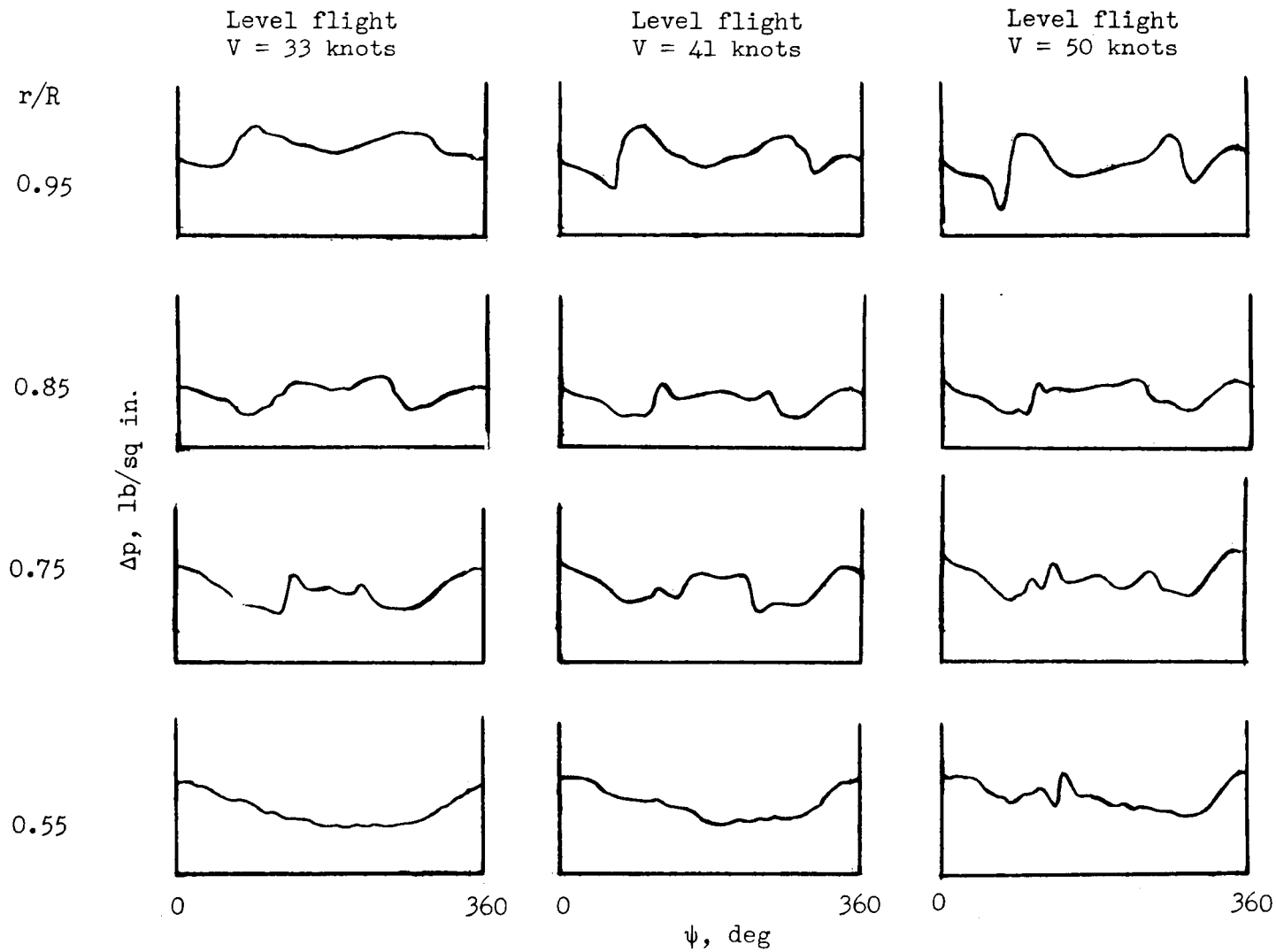

Figure 14.- Continued.

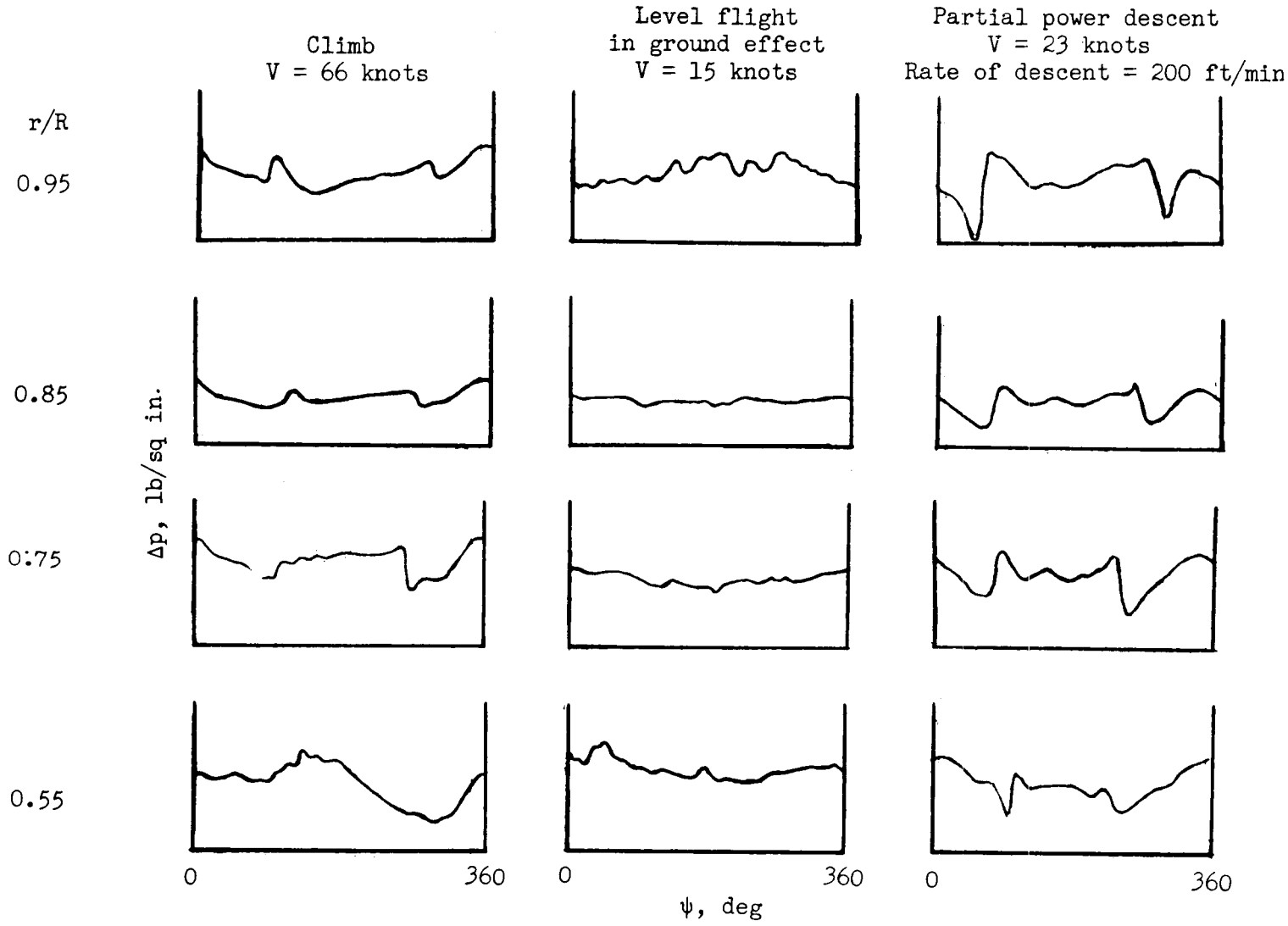

Figure 14.- Continued.

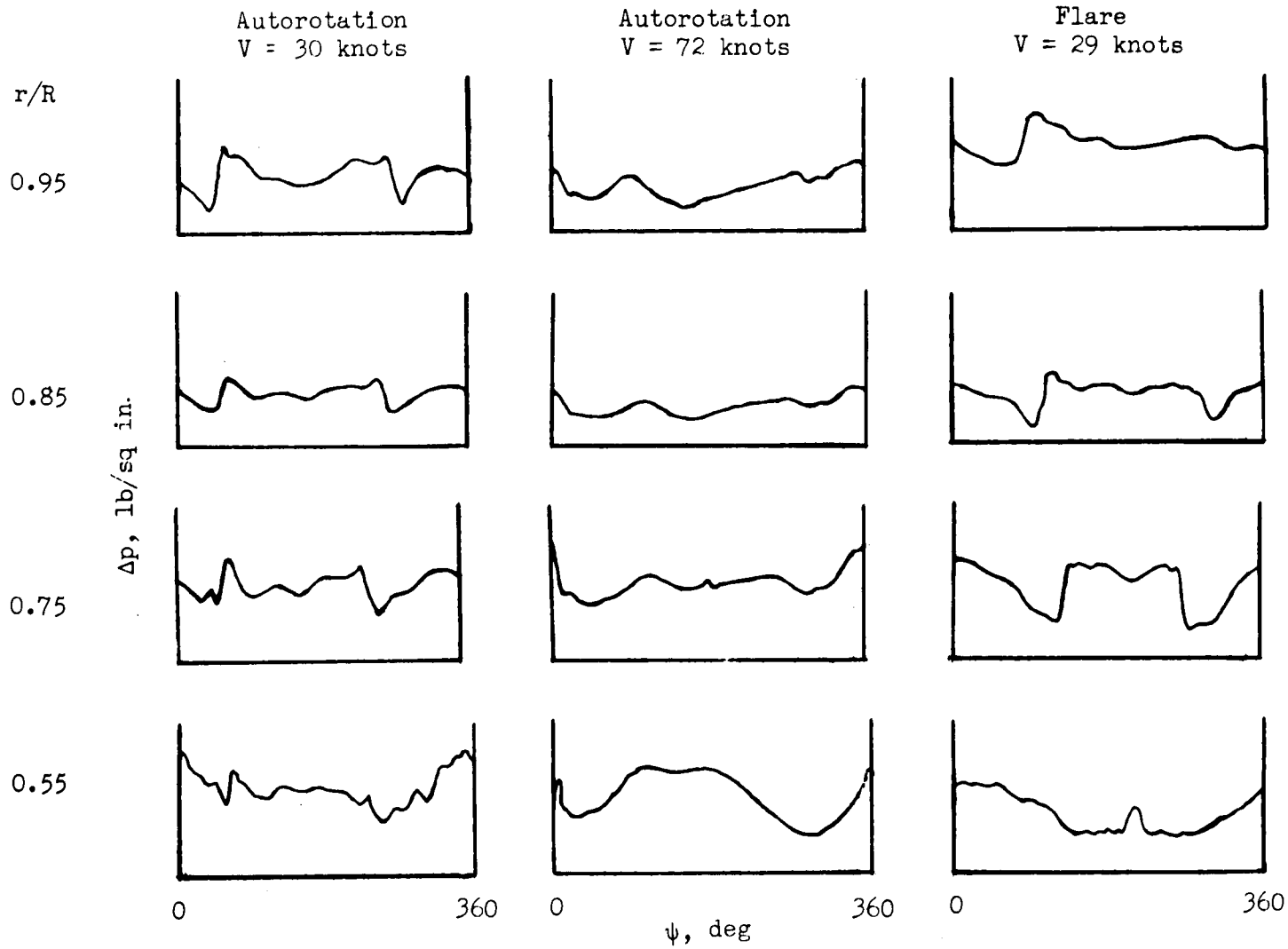

Figure 14.- Concluded.

NASA-Langley, 1963 L-3094